

HYDRODYNAMICS OF THE MISSION CANYON FORMATION
IN THE BILLINGS NOSE AREA,
NORTH DAKOTA

A Thesis

by

ALAN RAY MITSDARFFER

Submitted to the Graduate College of
Texas A&M University in
partial fulfillment of the requirements for the degree of
MASTER OF SCIENCE

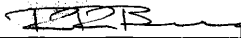
August 1985

Major Subject: Geology

HYDRODYNAMICS OF THE MISSION CANYON FORMATION
IN THE BILLINGS NOSE AREA,
NORTH DAKOTA

A Thesis
by
ALAN RAY MITSDARFFER

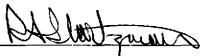
Approved as to style and content by:



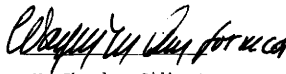
Robert R. Berg
(Chairman of Committee)



Patrick A. Domenico
(Member)



R. A. Startzman
(Member)



M. Charles Gilbert
(Head of Department)

August 1985

ABSTRACT

Hydrodynamics of the Mission Canyon Formation
in the Billings Nose Area,
North Dakota. (August, 1985)

Alan Ray Mitsdarffer, B.S., William and Mary
Chairman of Advisory Committee: Dr. Robert R. Berg

The Mission Canyon Formation in the Billings Nose area is a prolific reservoir which produces from a combination stratigraphic and structural trap. The reservoir section has been divided into three zones, designated "A", "B", and "C", based on log response. The section has undergone various degrees of dolomitization with the "A" zone having the greatest porosity and production.

Extrapolation of pressure buildups from drill stem tests (DST) provided fluid pressure data used in construction of regional potentiometric map which indicates flow to the east at low gradients of 10 ft/mi (1.9 m/km). A corrected potentiometric map based on fluid density variations shows a gradient across the field of 50 ft/mi (9.5 m/km) and flow to the northeast. Differences are due to a fresher water lens which has invaded the field area from the southwest creating a large salinity contrast across the field. The lens has been confirmed from salinities derived from DST water recoveries and well log

interpretations.

The calculated total oil column using an average potentiometric gradient of 50 ft/mi (9.5 m/km) is 1554 ft (474 m), which does not compare well to the observed column of 150 ft (46 m). The observed tilt of the oil-water contact is 25 ft/mi (5 m/km) to northeast in comparison to the calculated tilt of 127 ft/mi (24 m/km) to the northeast. These factors and the location of the oil accumulation imply that the oil accumulation is not in equilibrium with the existing hydrodynamic conditions.

The initial entrapment could not have taken place under the existing conditions but probably occurred under hydrostatic conditions. This was followed by hydrodynamic conditions with low gradients similar to that depicted by the regional map. The present hydrodynamic conditions result from the recent invasion of the field area by the fresher water lens. The oil accumulation will eventually be flushed from the area under these existing hydrodynamic conditions.

ACKNOWLEDGEMENTS

The author would like to thank all those involved in completion of this thesis. First and foremost, my thanks go to Dr. Berg, for his advice and assistance. His knowledge of the subject and overall attitude towards teaching are unsurpassed. My association with him, has improved me as a geologist as well as a person. He suggested the topic and provided financial assistance which was greatly appreciated.

The comments and interest shown by Dr. Domenico and Dr. Startzman is gratefully acknowledged. Their input as professors and committee members is appreciated. I would also like to thank Mike Walen and Patrick Petroleum for providing valuable information

Thanks to my fellow graduate students, especially Craig Eady, Tony McClain, Greg Bond, Kim Harriz, Pete George, Bill Blount, Pat Magee and others, who made the time at A&M enjoyable. Special thanks to Becky Bailey Lambert, Tom Dougless, and Scott Bicknell, who aided in the completion of the research in one form or another.

Finally, a special thanks to my wife, Terrie, for her support, aid and companionship without which I would not have been able to complete my studies.

TABLE OF CONTENTS

	Page
INTRODUCTION.....	1
Regional Geology.....	2
Structure.....	2
Stratigraphy.....	5
Production History.....	11
Methods.....	15
Previous Work.....	16
THEORETICAL BACKGROUND.....	20
Hydrodynamic Pressures.....	20
Potentiometric Surface.....	24
Fluid Pressure Measurements.....	25
BILLINGS NOSE AREA.....	29
Geology.....	29
Structure.....	29
Stratigraphy.....	30
Reservoir Properties.....	37
Production.....	42
Nature of the Trap.....	49
HYDRODYNAMICS.....	55
Fluid Pressures.....	55
Potentiometric Surface.....	64
Interpretation.....	84
OIL ACCUMULATION.....	93
Oil Source.....	93
Oil Migration.....	97

Oil Column Calculations.....	98
Capillary Oil Column.....	98
Hydrodynamic Oil Column.....	99
Oil-Water Contact.....	101
History of Oil Accumulation.....	104
CONCLUSION.....	109
REFERENCES CITED.....	111
APPENDICES.....	117
VITA.....	162

LIST OF FIGURES

Figure		Page
1	Index map of the Williston basin showing structure on top of the Mission Canyon Formation.....	3
2	Regional freshwater potentiometric map showing hydrostatic head for the Madison aquifer and location of study area.....	18
3	Regional salinity map for the Madison aquifer.....	19
4	Functional relationship between fluid pressure and dimensionless time log ($T+t/t$) for a typical DST which indicates steady state buildup (AB) extrapolated to an original reservoir pressure (p_i)...	27
5	Structure map on top of Mission Canyon Formation in the Billings Nose field area showing gently northward plunging anticlinal structure.....	32
6	Billings Nose field area showing structure on gamma marker within the reservoir section (see Fig. 8).....	34
7	Regional isopach of the Nesson Anhydrite showing increasing thickness to the southeast and pinchout to the northwest..	36
8	Representative well log in the Billings Nose field area showing division of Mission Canyon reservoir section into the "A", "B" and "C" zones.....	38
9	Porosity, permeability, and fluid saturations for the Mission Canyon reservoir section in the Hamill 3-27 core	40
10	Cross plot of permeability and porosity from the Hamill 3-27 core (Fig. 9) showing bi-modal distribution of porosity	41

11	Net thickness of porosity greater than 8 percent in the "A" zone (Fig. 8) in the Billings Nose field area.....	44
12	Net thickness of porosity greater than 8 percent in the "B" zone (Fig. 8) in the Billings Nose field area.....	46
13	Initial production map for the Mission Canyon in the Billings Nose field area...	48
14	Water production map for the Mission Canyon in the Billings Nose field area showing water production as a percentage of total initial production.....	51
15	Regional cross section from Rough Rider field to Fryburg field showing the relationship of production to stratigraphic position of the porous zones.....	53
16	Pressure buildups for the initial (ISI) and final (FSI) shutin periods in the Al-Aquitaine US 1-22 showing the extrapolated original pressure (p_o).....	57
17	Pressure buildups for the initial (ISI) and final shutin (FSI) periods in the Shell Government 1H-20 showing the extrapolated original pressure (p_o).....	59
18	Pressure buildup for the final shutin (FSI) period in the Chambers State 1-23 showing layered character.....	61
19	Pressure buildup for the final shutin (FSI) period in the Apache Federal 1-5 showing layered character and extrapolated original pressure (p_o).....	62
20	Pressure buildup for the initial shutin (ISI) period in the Farmers Federal 4-33 showing layered character, extrapolated original pressure (p_o) and probable original pressure (p_i).....	63
21	Pressure buildup for the final shutin (FSI) period in the Patrick Federal 2-32 showing effect of a barrier.....	65

22	Regional freshwater potentiometric map for the Mission Canyon Formation.....	66
23	Plot showing pressure as a function of elevation for representative Mission Canyon, Bakken, Midale and Ratcliffe tests in the Billings Nose area.....	68
24	Regional salinity map from DST data for the Mission Canyon showing strong salinity gradient to the northeast.....	70
25	Regional temperature map from DST data...	72
26	Regional corrected potentiometric map showing strong gradient to the northeast.	75
27	Pickett plot for Patrick Hamill 3-27 showing water resistivity (R_w) of 0.09 ohm-m and variations in water saturation (S_w).....	78
28	Pickett plot for Tenneco 3-25 showing water resistivity (R_w) of 0.054 ohm-m and variations in water saturation (S_w)..	79
29	Pickett plot for Tenneco Stuart 3-7 showing water resistivity (R_w) of 0.018 ohm-m and variations in water saturation (S_w).....	80
30	Water resistivity map from log interpretation (Figs. 27, 28, 29) in the Billings Nose field area showing location of high resistivity lens.....	82
31	Billings Nose field area salinity map from water resistivity values (Fig. 30)..	86
32	Corrected Billings Nose field area potentiometric map showing strong gradient to the northeast.....	88
33	Billings Nose field area freshwater potentiometric map.....	90
34	Diagrammatic cross section in Billings Nose field area showing water salinity change in relation to porosity zones.....	92

35	Lopatin diagram for the Bakken Shale in the Billings Nose area showing burial history and onset of oil generation.....	95
36	Apparent oil-water contact map for the Billings Nose field showing gentle tilt to the northeast.....	103
37	Diagrammatic cross section through center of Billings Nose field area showing oil accumulation under hydrostatic conditions (A) and hydrodynamic conditions (B).....	106

LIST OF TABLES

Table		Page
1	Mississippian Stratigraphy for the Williston Basin.....	7
2	Madison nomenclature in the Williston Basin and surrounding areas.....	12
3	Conversion of salinities to pressure gradients.....	74
4	Values used in correction of potentiometric maps.....	76
5	Conversion of water resistivities to salinities.....	83
6	Calculation of time-temperature index (TTI) for burial history of Bakken Shale in Figure 35.....	96
7	Summary of oil column calculations and rock and fluid properties for the Mission Canyon Formation.....	100

INTRODUCTION

The theory and application of hydrodynamic flow of groundwater to oil accumulation was originated by Hubbert (1940, 1953). His theory that subsurface waters can be either a dynamic or static system has changed the concepts of oil and gas migration and accumulation. An understanding of the hydrodynamic regime in an area may be as important to successful exploration as structure and stratigraphy. Downdip flow has been shown to increase the oil column in a stratigraphic trap (Hubbert, 1953). Berg (1972, 1975) developed a method for the calculation of the oil column in a stratigraphic trap under hydrostatic or hydrodynamic conditions. A knowledge of both the fluid and rock properties is essential to these calculations.

The Billings Nose area contains one of the numerous Mission Canyon reservoirs in the Williston basin. The Mission Canyon Formation is part of a major aquifer system which covers most of the northern Great Plains, including the Williston basin. The purpose of this study is to determine the existence of hydrodynamic flow in the Billings Nose area and evaluate its effect on oil accumulation.

This thesis follows the format and style of the American Association of Petroleum Geologists Bulletin.

Regional Geology

Structure

The Williston basin is an intracratonic basin that forms a slightly irregular, round depression in the western edge of the Canadian shield. The basin encompasses approximately 250,000 sq mi (647,500 sq km) and occupies much of North Dakota, eastern Montana, southern Saskatchewan, and parts of South Dakota and Manitoba. The major structural features which bound the basin are the Sweetgrass arch to the west, the Black Hills to the southwest, and the Sioux arch to the south. The Canadian shield bounds the basin on the northeast and east, while to the northwest in Saskatchewan the basin merges with the Moose Jaw syncline.

The Williston basin is characterized by gentle basinward dips, lack of abrupt facies changes, and a generally uneventful tectonic history (Bridges, 1978). Prior to extensive petroleum exploration the basin was generally considered a simple depressed saucer with two positive structures, the Nesson anticline in northwestern North Dakota, and the Cedar Creek anticline in southeastern Montana (Fig. 1). Smaller, more subtle structures such as the Poplar dome, Billings and Little Knife anticlines were delineated, with the increase in drilling and seismic

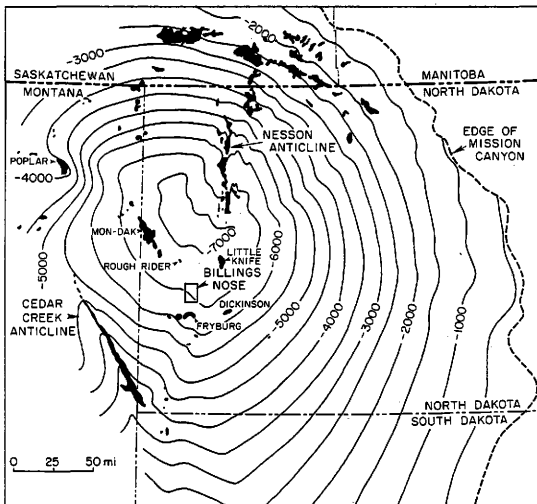


Figure 1. Index map of the Williston basin showing structure on top of the Mission Canyon Formation. Also shown are the major oilfields and structures in the basin. Contour interval is 500 ft (152 m). Modified from Hansen (1972).

exploration programs.

It appears that intrabasinal structures have been controlled by movement of basement blocks. The structural trends within the Williston basin reflect both the north and northwest structural grain of the Rocky Mountain province (Gerhard et al, 1982). The Nesson, Billings and Little Knife anticlines are north trending, while the Cedar Creek anticline and Poplar dome are dominantly northwest trending. Gerhard et al, (1982) have postulated that left-lateral shearing was not only responsible for the change in the structural grain of the Rockies but the formation of basement-rooted faults within the Williston basin as well. Thomas (1974) and Brown (1978) have used a wrench fault system to explain basin geometry and structure. This theory is derived from lineament patterns, which are considered to be controlled by the location of fault-bounded basement blocks.

The Billings Nose is located on the southern flank of the basin in southwestern North Dakota. The regional dip in the area is approximately 30 ft/mi (5.7 m/km) to the north. The Billings Nose itself is a gently northward plunging structure which is broad to the south but narrow to the north. The structure had an effect on sedimentation patterns as early as the Late Ordovician (Carroll, 1978).

Stratigraphy

The sedimentary rocks in the deepest part of the Williston basin reach an approximate thickness of 16,000 ft (4,877 m) (Gerhard et al, 1982) and rocks from all periods of the Phanerozoic have been preserved. The Paleozoic strata are predominately carbonate, while the Mesozoic and Cenozoic strata are clastics.

The record begins during the Late Cambrian when the area of the Williston basin was transgressed by shallow marine seas from the west. At this time, the basin was probably a large embayment in the Cordilleran shelf (Lochman-Balk, 1972). The Middle Ordovician through Silurian record is one of transgression, sedimentation, and regression which is repeated throughout the Paleozoic. It was during the Ordovician that the Williston basin became a well defined structural feature. Foster (1972) has proposed that the basin's marine connection was from the southwest during this time.

The Devonian is marked by uplift which broke the marine connection to the southwest and tilted the basin northward. This allowed transgression from the north and possibly the west, and the basin became a part of the larger Devonian seaway in Canada. Another reorientation of the seaways took place during the Late Devonian, so that during the Mississippian the connection was to the west

through the Central Montana trough (Bjorlie and Anderson, 1978). Cycles of transgression, sedimentation, and regression continued through most of the Mississippian.

The Pennsylvanian orogenic events in the craton and Rocky Mountain region brought a change in the pattern of sedimentation within the basin. The marine connection from the west still existed, but was restricted by the spread of clastics into the basin from the southwest, southeast and northeast. The remainder of Paleozoic record, as well as the Mesozoic and Cenozoic is dominated by clastic facies, interspersed evaporites and few carbonates.

The Mississippian sediments in the central basin reach a thickness in excess of 2,500 ft (762 m) (Table 1). The configuration of the basin during that time was very similiar to the present basin. Uplift occurred during the latest Devonian and earliest Mississippian time exposing Devonian strata along the basin margins (Sandberg, 1964). This event was not only responsible for the formation of an angular unconformity along the eastern margin of the basin, but caused a change in the marine connection from the north to the west. The uplift had no affect on the central part of the basin where sedimentation continued.

Mississippian sedimentation began with the deposition of sediments during a transgression. The Bakken Formation is the relatively thin, basal Mississippian unit which lies

Table 1. Mississippian Stratigraphy for the Williston Basin.

Age	Group	Formation
		Heath
	Big Snowy	Otter
		Kibbey

Mississippian		Charles
	Madison	Mission Canyon
		Lodgepole

		Bakken

unconformably on the Devonian sediments along the basin margins. The contact in the central basin area appears to be conformable. The Bakken Formation consists of fine-grained clastics, predominately shale, which were deposited during a major transgression. The Bakken can be divided into three members, which are a Lower Shale Member, a Middle Silstone Member and an Upper Shale Member (Meissner, 1978). The total formation thickness reaches a maximum of 140 ft (43 m) in the central basin.

A gradual transgression continued throughout Bakken time as evidenced by the onlapping relationship of the Bakken members (Webster, 1984). The upper and lower shales are black and organic-rich, which required anoxic conditions for deposition. The depositional environment of these shales is problematic but restricted basin conditions must have existed during their deposition.

The Mississippian transgression continued after the deposition of the Bakken and normal marine conditions returned. This was a time of predominately marine carbonate deposition which was followed by a gradual reduction in circulation that produced cyclic carbonate and evaporite deposition (Carlson and Anderson, 1965). This sequence of deposits is the Madison Group, which has a thickness of 2,000 ft (610 m) in the basin center. Three formations compose the Madison Group and these are the

Lodgepole, Mission Canyon and Charles.

The basal Madison unit is the Lodgepole Formation which conformably overlies the Bakken. The Lodgepole is dominated by dark colored mudstones which represent deep basin and slope deposition. A variety of other facies were developed along the basin margins, such as mudmounds, oolitic banks and lagoonal deposits (Heck, 1978).

Maximum transgression occurred near the end of Lodgepole or early during Mission Canyon deposition (Gerhard et al, 1982). The Mission Canyon Formation consists of nearshore and coastal facies, containing grainstones, packstones and mudstones with varying degrees of dolomitization. The most shoreward facies often contain sequences of anhydrite (Altschuld and Kerr, 1982). The Mission Canyon forms the major reservoirs in the Billings Nose area. The Charles Formation was deposited over the Mission Canyon as regression occurred and the Charles consists primarily of halite and anhydrite, which are thickest in the basin center.

The Mississippian record was brought to a close with the deposition of the Big Snowy Group, which conformably overlies the Charles Formation. The Big Snowy Group has been divided into three formations which, in ascending order are: Kibbey, Otter and Heath. The Kibbey is composed of shale, limestone and sandstone, whereas the Otter is

shale and limestone, and the Heath Formation is composed of grey and black shale. The sediments of the Big Snowy Group were deposited in alternating restricted and normal marine environments.

The Madison Group nomenclature in the Williston Basin and surrounding areas can be confusing. The Madison was originally defined from outcrops in Montana and was later given group status (Kupecz, 1984). The Lodgepole and Mission Canyon Formations were named for canyons in the Little Rocky Mountains of Montana. The Charles Formation was named from a subsurface section and was originally the basal unit of the Big Snowy Group. Each of the formations represented distinct facies but as subsurface work progressed, an interfingering relationship was recognized (Carlson and Anderson, 1965). The formations are largely time-transgressive so they appear at lower stratigraphic levels toward the edges of the basin.

These relationships led to revisions of the nomenclature based on well log marker beds. These beds were thought to be time parallel (Fuller, 1956), and the Madison was divided into six time-stratigraphic units. These units were called beds and, in ascending order, are the Souris Valley, Tiltston, Frobisher-Alida, Midale, Ratcliffe, and Poplar. All the beds can be recognized near the basin margins but in the central basin this is not the

case. The North Dakota Geological Society (Smith, 1960) referred to these units as intervals and redefined some of the markers (Table 2). Informal members have been created based on marker beds and have been used by petroleum geologists in the basin. This study will use the informal members where applicable, but the group, formation nomenclature will dominate.

Production History

The Williston basin is a major producer of oil and gas. Production has been established in a number of zones ranging in age from the Ordovician to the Cretaceous. Mississippian production is the greatest with the Madison reservoirs being the most prolific (Proctor and Macauley, 1956).

The first oil in the basin was discovered in Montana along the Cedar Creek anticline in 1936, but was noncommercial (Hamke et al, 1966). The discovery of Devonian reef production in Alberta in the late 1940s played a role in the development of commercial oil in the Williston basin. This Devonian play was extended across Saskatchewan, Manitoba and into North Dakota (Lindsey, 1954), and oil was first found in producible quantities in Manitoba in early 1951 (Lindsey, 1954). The first commercial oil discovery in the United States portion of

Table 2. Madison nomenclature in the Williston Basin and surrounding areas.

Standard	Saskatchewan Geological Society Fuller, 1956 (BEDS)	North Dakota Geological Society Smith, 1960 (INTERVAL)
	POPLAR	POPLAR
CHARLES FORMATION	RATCLIFFE	RATCLIFFE
		Midale (sub-interval)
	MIDALE	Rival (sub-interval)

	PROBISHER	PROBISHER
MISSION CANYON	-ALIDA	-ALIDA
FORMATION	TILSTON	TILSTON

LODGEPOLE FORMATION	SOURIS VALLEY	BOTTINEAU

the Williston basin was later the same year. The discovery well, the Clarence Iverson No. 1, was on the Nesson anticline. The well was originally completed for Silurian and Devonian production but was later recompleted in the Madison (Gerhard, et al, 1982). The Madison became the primary target for development of the anticline.

This discovery led to an explosion of activity and success. Early drilling was largely confined to the major structures of the basin, the Nesson, Cedar Creek and Poplar anticlines. The Madison reservoirs dominated with production from Ordovician, Silurian, and Devonian reservoirs as well. The first production in the vicinity of the Billings Nose came in 1953, with the discovery of the Fryburg field to the south. Production was developed in the Madison, as well as in the Mississippian Heath Formation.

The success of the Madison stratigraphic and unconformity plays in North Dakota and Canada in the middle to late 1950s rekindled exploration interest (Carlson and Anderson, 1965). The Fryburg trend was expanded at this time with the discovery and development of the Scoria and Dickinson fields. The Rough Rider field, which lies to the north of the Billings Nose, was discovered in 1959 with Madison production. Minor Madison production was also established at the Blacktail field in 1960. The Medora

field was discovered in 1964, along the Fryburg trend.

The 1960s and early 1970s was a time of decreased activity in the basin. This came to an end with OPEC's embargo and the Red Wing Creek field discovery. OPEC's actions made it more profitable to explore, while the thick pay sections and high productivity wells of the Red Wing Creek field set off a wave of leasing in the basin (Gerhard et al, 1982). This combination led to a dramatic rise in drilling.

This recent activity has produced many new fields as well as expanding older ones. In 1977, the Mondak field was discovered along the Montana - North Dakota border, as well as the Little Knife field, which lies just to the northeast of the Billings Nose area. The Madison is the reservoir in both fields. Also in the Billings Nose area, Madison production was established at the Elkhorn Ranch field in 1974. Drilling activity was moderate until the 1978 discovery by Tenneco of the Mission Canyon and Devonian reservoirs at the Four Eyes field (Altschuld and Kerr, 1982). Subsequent drilling defined the TR, Big Stick, Tree Top, and Whiskey Joe fields which with Four Eyes have been combined into one large producing area known as the Billings Nose. Approximately 42 million barrels of oil has been produced from the Mission Canyon Formation in this area (as of January, 1983) (Rygh, 1983).

Methods

The study of the hydrodynamics of an aquifer system requires the use of pressure data. Drill-stem tests can provide pressure, depth and temperature relationships for an aquifer. Adequate drill-stem test data for the Billings Nose area and surrounding thirty townships are available from industry sources (Appendix A).

The evaluation of drill-stem test pressure buildups was accomplished using a Hewlett-Packard 9820A programmable calculator equipped with plotter and tape drive (Larberg, 1976). Interpretation of the pressure buildups was made in accordance with the Horner (1951) method to determine original fluid pressures. Hydrostatic heads were calculated throughout the region using these pressures and a constant pressure gradient of 0.433 psi/ft (Appendix B). An API gravity of forty was used in correction of oil column pressures to those in the water column. A regional potentiometric map was constructed using only the reliable hydrostatic heads.

The Pickett (1966) crossplot method of well log interpretation was used to determine the resistivities of the formation waters which were mapped in the field area. This resistivity map was transformed to a salinity map with the use of Schlumberger charts and field temperatures. The field potentiometric map was corrected for water density

variations through the use of the salinity map. An oil-water contact map was constructed from Pickett crossplot interpretations, in conjunction with well completion data.

Well logs were used to construct net isopachs, a structure map of a marker bed and cross sections in the field area. Information from completion cards was used to construct initial production and water production maps.

Previous Work

The Williston basin does not possess the rugged topography and steep dips of the intermontane basins that are noted for hydrodynamic influence on oil accumulations (Berg, 1976, Stone and Hoeger, 1973, Lin, 1981). These basins have moderate to strong hydrodynamic gradients, in contrast to the low gradients of the Williston basin. The recharge areas for the Madison Group include the Black Hills of South Dakota, the Bighorns of Wyoming, the Little Rocky Mountains and associated highlands of central Montana (Fish and Kinard, 1959).

Hydrodynamic flow was considered as a possible cause for the observed tilted oil-water contact for the Nottingham field in Saskatchewan, but the direction of tilt was opposite to flow and was thus explained by lithology changes (Eddie, 1958). Despite the low gradients,

hydrodynamic flow does have an affect on oil accumulations within the basin. Murray (1959) illustrated that the tilted oil-water contacts observed in the Madison reservoirs in the North Tioga (Nesson anticline) and Poplar fields (Fig. 1) were due to hydrodynamic flow.

The Madison Group is a major aquifer system and the USGS has recently undertaken a thorough geologic study of the unit. The purpose of the study was to evaluate the Madison Group as a possible source for large quantities of water necessary for a proposed coal-slurry pipeline. The study area includes Montana, Wyoming, Nebraska, Norh Dakota and South Dakota, with major emphasis on the recharge areas surrounding the Black Hills and Big Horns.

A number of hydrologic papers have originated from the study. A regional potentiometric map (Miller and Strausz, 1980) has been published for the Madison aquifer and shows hydrodynamic flow in the Billings Nose area (Fig. 2) with a gradient of approximately 10 ft/mi. This map is of limited use due to the lack of control and no corrections for water density variations. Downey (1984) modeled flow in the Madison aquifer and presented a regional salinity map (Fig. 3), which shows salinities ranging from less than 100,000 ppm to greater than 300,000 ppm in the study area.

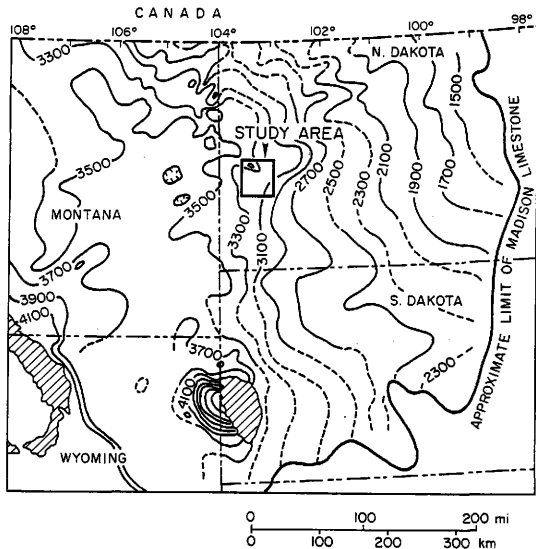


Figure 2. Regional freshwater potentiometric map showing hydrostatic head for the Madison aquifer and location of study area. Contour interval is 200 ft (61 m). Modified from Downey (1984), Miller and Strausz (1980).

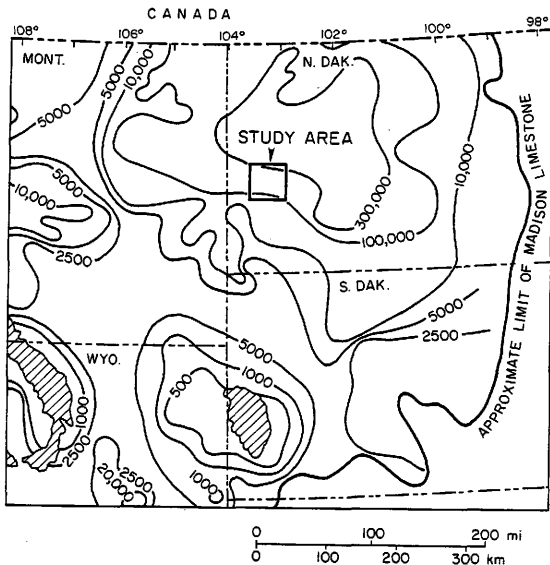


Figure 3. Regional salinity map for the Madison aquifer. Location of study area is shown. Contour values in parts per million; interval varies as indicated. Modified from Downey (1984).

THEORETICAL BACKGROUND

The hydraulic theory for oil and gas migration and accumulation was proposed by Munn (1909) in 1909. According to Munn's theory oil and gas migrated with the flow of water and was entrapped in any position where resistive forces overcame the impelling force of the moving water. The anticlinal theory was the accepted model for oil accumulations at that time and is still generally accepted. The fundamental principle of the anticlinal theory, is that oil and gas will accumulate at the highest possible position within the reservoir (Levorsen and Berry, 1967). Hubbert (1953) stated that this is a special case and valid only when ground water is in hydrostatic equilibrium. The hydrodynamic flow of groundwater can play an important role in the entrapment of oil and gas in stratigraphic and structural traps.

Hydrodynamic Pressures

The flow of groundwater in the subsurface can best be understood in terms of potential. Hubbert (1940) has defined potential as a physical quantity, capable of measurement everywhere in a flow system, whose properties are such that flow occurs from regions of higher values to those of lower values regardless of direction. The potential for water, I , can be expressed as follows:

$$I = Zg + P/D = gh \quad (1)$$

where Z is the elevation with respect to a datum, P is the gauge pressure at that elevation, D is the fluid density, g is the acceleration due to gravity, and h is the hydrostatic head. The fluid potential at any point in the aquifer is the hydrostatic head at that point multiplied by the acceleration due to gravity. If gravity is assumed not to vary with elevation in the vicinity of the earth's surface, then hydrostatic head, h , and fluid potential, I , are approximately the same. If fluid potential is energy per unit mass, then hydrostatic head is energy per unit weight (Freeze and Cherry, 1979).

Hydrostatic head can be defined as the height that a column of water will rise above a datum in response to formation pressure. Dividing equation (1) through by g yields:

$$h = Z + P/Dg \quad (2)$$

where Z is the elevation with respect to a datum, usually sea level, P is the pressure measured at that elevation, D is the fluid density, and g is the acceleration due to gravity. Head fits Hubbert's definition of potential, in

that it is a physical measurable quantity, and flow occurs from regions of higher head to those of lower head. The flow of groundwater will occur in response to variations in head, and if the head is everywhere the same, then the fluid is at rest or static.

Oil and gas must migrate through the water saturated medium of the subsurface. The hydrodynamic flow of groundwater has significant affect on the migration and entrapment of oil and gas. Hubbert (1953) has shown that oil and gas accumulations will exhibit a tilted interface where hydrodynamic flow exists. The angle of this interface can be expressed as

$$\tan Q = dz/dx = D_w / (D_w - D_o) * (dh/dx) \quad (3)$$

where Q is the angle of inclination, dz/dx is the slope of the oil-water interface, dh/dx is the horizontal head gradient, and $D_w / (D_w - D_o)$ is an amplification factor (Willis, 1961) based on the respective densities of water and oil. The tilting of the oil-water interface will occur in stratigraphic or structural traps, and may cause an increase or decrease in the amount of oil trapped under hydrostatic conditions.

Capillary pressures are effective in trapping oil in stratigraphic traps. Berg (1972, 1975) has developed a

method for calculating the oil column that can be trapped due capillary pressure differences. The capillary oil column, Z_c , can be calculated as follows:

$$Z_c = 2t (1/R_t - 1/R_p) / g(D_w - D_o) \quad (4)$$

where t is the interfacial tension between oil and water, R_t is the radius of pore throats in the barrier rock, R_p is the radius of pores in the reservoir, g is the acceleration due to gravity, and D_w and D_o are the densities of water and oil respectively under subsurface conditions (Berg, 1975). This calculation is valid under static conditions. The additional oil column trapped by hydrodynamic flow may be calculated as follows:

$$Z_o = D_w / (D_w - D_o) (dh/dx) x_o \quad (5)$$

where x_o is the horizontal width of the oil accumulation.

The total oil column, Z_{ot} , can be derived by combining the capillary oil column and hydrodynamic column as:

$$Z_{ot} = [2t [(1/R_t) - (1/R_p)] / g(D_w - D_o)] \\ \pm [D_w / (D_w - D_o)] * (dh/dx) * x_o \quad (6)$$

where the sign of the hydrodynamic column is determined by

the direction of flow in relation to the barrier (Berg, 1975). Updip flow would decrease the column, while downdip flow would increase it.

Potentiometric Surface

The study of the regional flow pattern of an aquifer requires the use of a potentiometric surface. Any point on the surface is a measure of the fluid potential with respect to its position and pressure within the aquifer (Hubbert, 1953). A potentiometric surface or map can be constructed by contouring heads of equal value for a specific aquifer. Flow will occur normal to the head contours, from high to low head or from high to low potential.

The empirical law which is used to analyze flow in a porous medium is based on the experimental work of Darcy (1856). The Darcy equation relates flow discharge (Q), and the physical properties of the fluid and aquifer as follows:

$$Q = kA (Dg/u) (dh/dx) \quad (7)$$

where k is the formation permeability, A is the cross-sectional area, u is fluid viscosity, D is the fluid density, g is the acceleration due to gravity, and dh/dx is

the horizontal head gradient. If flow (Q) and the cross-sectional area (A) are assumed to remain constant, then there is an inverse relationship between permeability (k) and the head gradient (dh/dx). This relationship can be useful in the interpretation of potentiometric maps. The porous and permeable parts of an aquifer will be represented by low head gradients or widely spaced head contours. A steep head gradient or closely spaced contours may be indicative of a low permeability zone, and thus a barrier to oil migration.

A petroleum trap as defined by Hubbert (1953) is a low-energy or low-potential region which is surrounded by higher energy areas, or jointly by impermeable barriers and higher energy areas. Applying this definition, one would expect to find petroleum reservoirs associated with potentiometric lows or areas with low head gradients.

Fluid Pressure Measurements

The drill-stem test is a temporary completion of a well, that is designed to evaluate the productivity potential of a formation and provide pressure data. A properly run and interpreted drill-stem test can provide a range of geologic and hydrologic information.

The use of the Horner (1951) method of drill-stem test evaluation requires several assumptions: 1) the formation

is homogeneous and infinite in extent, 2) flow is radial and Darcy's law applies, 3) single phase flow only, and 4) "steady-state" or equilibrium conditions exist during the final stages of pressure buildup. The buildup equation derived by Horner (1951), relates various rock and fluid properties with flow as follows:

$$P_w = P_i - [(162.6QuB)/(kh)] \log [(T+t)/t] \quad (8)$$

where P_w is the fluid pressure in the well bore, P_i is the maximum reservoir pressure, Q is the flow rate, u is the fluid viscosity, B is the formation volume factor, k is the formation permeability, h is the formation thickness, T is total flow time, and t is the incremental shutin time. The maximum or original reservoir pressure must be obtained by the extrapolation of the final stages of the pressure buildup to $(T+t)/t = 1$ or infinite shutin time (Fig. 4). This pressure, along with the gauge depth, is used in the hydrostatic head calculation.

Certain terms in equation (8) become constant, through the application of the previous assumptions. These are the fluid properties (u , B), the formation properties (k , h) and the flow rate (Q). Another constant (M) can be derived as follows:

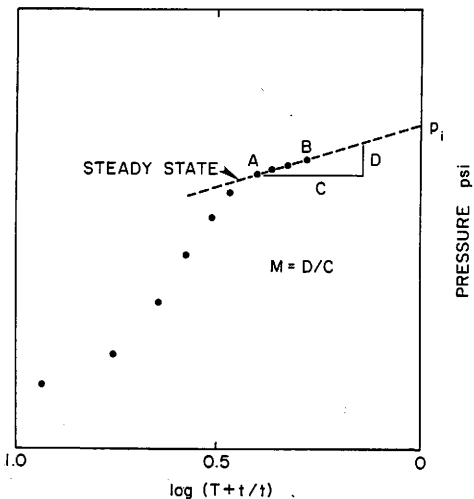


Figure 4. Functional relationship between fluid pressure and dimensionless time $\log (T+t/t)$ for a typical DST which indicates steady state buildup (AB) extrapolated to an original reservoir pressure (p_i).

$$M = 162.6 \text{ QuB/ (kh)} \quad (9)$$

The constant (M) also represents the slope of the "steady-state" extrapolation line (Fig 4). The formation permeability can be calculated by rearranging equation (9) as

$$k = 162.6 \text{ QuB/ (hM)} \quad (10)$$

The parameters of flow rate (Q), and fluid properties (u, B) may be obtained from the drill-stem test, while M may be obtained from the pressure buildup. The formation thickness (h) can be estimated from well logs. The original reservoir pressure and formation permeability can be obtained from any reliable drill-stem test.

BILLINGS NOSE AREA

The Billings Nose area is located on the southern flank of the Williston basin, in northern Billings County, North Dakota. The principal reservoir is the Mission Canyon Formation, as it is in many of the other fields of the central basin, Little Knife, Mon-Dak, and Rough Rider (Fig. 1). A well to a deeper objective led to discoveries in the Mission Canyon and Devonian Duperow Formations at the Four Eyes field in 1978. As drilling progressed other fields were defined: TR, Big Stick, Tree Top, and Whiskey Joe, which were later combined into one large producing area covering over 30,000 acres (Altschuld and Kerr, 1982).

Over 150 producing wells have been completed in the Mission Canyon Formation in the Billings Nose area. Other wells have also been completed in the Mississippian Bakken and Devonian Duperow Formations. As of January, 1983, the cumulative production from the Mission Canyon was approximately 42 million barrels of oil.

Geology

Structure

The Billings anticline is a gently northward plunging feature that is broad to the south but narrows to the north. This pattern is reflected in the structure as

mapped on the top of the Mission Canyon Formation (Fig. 5), as well as on the gamma marker within the reservoir section (Fig. 6). Structural closure is minimal, and the beds dip to the north at approximately 25 ft/mi, to the east at approximately 50 ft/mi, and to the west at approximately 20 ft/mi. The present structure is the result of deformation that occurred during the Laramide orogeny (Kupecz, 1984).

Sedimentation patterns have been effected by the anticline as early as the Ordovician (Carroll, 1978). Thinning of Mississippian sediments over the present structure suggests that structural control was present during Mission Canyon deposition (Kupecz, 1984). The effect on the Mission Canyon Formation was limited, although there appears to be a relationship between structure and facies patterns. Embayments in the paleoshoreline may have been structurally controlled and some facies tend to follow the present structural pattern.

Stratigraphy

The Mission Canyon Formation is a regressive carbonate to anhydrite sequence, with shoaling upward cycles in the carbonate phase (Lindsay and Roth, 1982). This sequence is similar to the lime mud to sabka cycle described by Wilson (1975). The carbonate rock types are dominantly mud supported, with minor grain supported fabrics. The entire

Figure 5. Structure map on top of Mission Canyon Formation in the Billings Nose field area showing gently northward plunging anticlinal structure. Contour interval 50 ft (15 m). Modified from Walen (pers. comm., 1983).

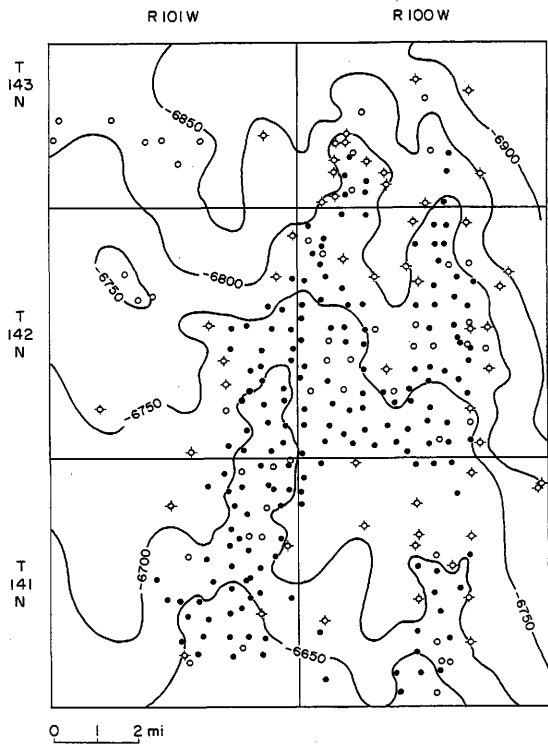
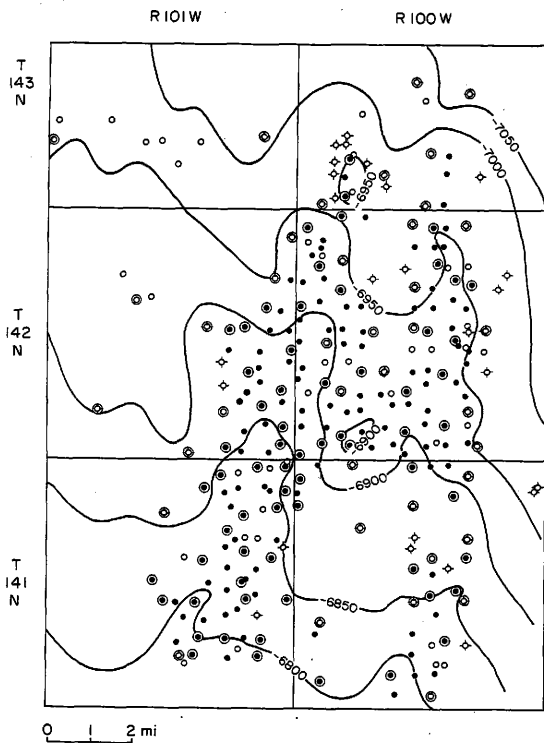


Figure 6. Billings Nose field area showing structure on gamma marker within the reservoir section (see Fig. 8). Note gently northward plunging anticlinal structure and similarities to Figure 5. Contour interval is 50 ft (15 m); circled wells mark points of control.



sequence has undergone varying degrees of dolomitization.

A shoaling upwards cycle in the Mission Canyon contains a basal open marine facies, a shoreline facies, and a supratidal facies (Altschuld and Kerr, 1982). The open marine facies represents normal, shallow-water carbonate sedimentation. The texture is one of thorough bioturbation, which is similar to the underlying Lodgepole Formation. There are also layers of crinoidal grainstones, and fossiliferous packstones, with occasional anhydrite nodules, which mark partial or incomplete regressive cycles.

The Mission Canyon tidal flat contained channels, levees and supratidal ponds similar to the Andros Island tidal flat described by Shinn et al, (1969). A sabka moved basinward to the northwest, replacing the tidal flat. Only one major anhydrite unit developed, which is named the Nesson Anhydrite. It is in excess of 120 feet (37 m) thick, but thins and pinches out to the northwest (Fig. 7).

The shoreline facies represents subtidal and intertidal deposition. It is bioturbated, with pellets and skeletal debris. This facies is often dolomitized and forms the main reservoir in the Billings Nose area. The distinctive supratidal facies, with desiccation cracks, stromatolites, birdseye and fenestral fabrics, overlies the shoreline facies.

In most tidal-flat sequences, the supratidal facies is dolomitized, but in this area it is limestone, which suggests that early cementation had taken place, reducing porosity and permeability. The dolomitizing fluids would have had limited access, and thus little affect, on the supratidal sediments. The underlying sediments of the shoreline facies, with porosity and permeability intact, have undergone the greatest amount of dolomitization. The mud-supported parts of the open marine facies have undergone various degrees of dolomitization.

The reservoir section in the Billings Nose area has been divided into 3 zones designated "A", "B", "C" based on log characteristics (Fig. 8). The gamma marker within the "B" zone is a silty dolomite and is continuous throughout the region. Kupecz (1984) has proposed that this is a dust storm deposit and thus a time marker. The "B" and "C" zones are also continuous, while the "A" zone pinches out to the southeast, and is replaced by the Nesson Anhydrite.

Reservoir Properties

Diagenetic processes, as opposed to the primary rock properties of composition and texture, control the presence of porosity and permeability. Dolomitization is responsible for the development of good reservoir

TENNECO
STUART 3-7
SW NE 7-142N-100W

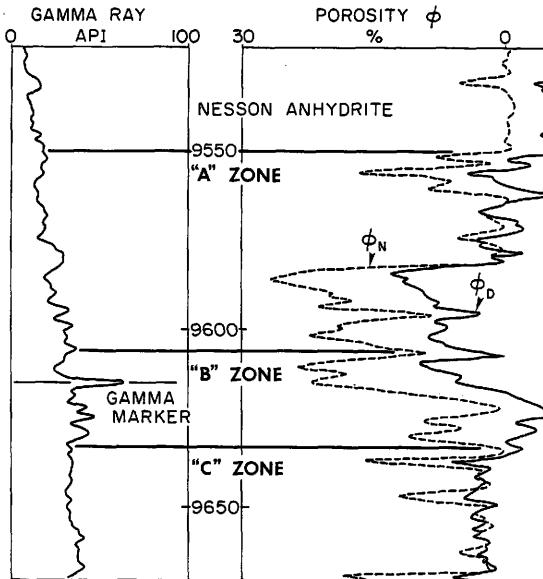


Figure 8. Representative well log in the Billings Nose field area showing division of Mission Canyon reservoir section into the "A", "B" and "C" zones. Also shown are the Nesson Anhydrite (Fig. 7) and gamma marker (Fig. 6).

character. There is a relationship between texture and dolomitization, in that mud supported sediments were preferentially dolomitized; except where early cementation had taken place. Fracturing may also play a role in porosity and permeability development.

The core analysis from the Hamill 3-27 well shows the cyclic nature of porosity development. (Fig. 9). The "A" zone has an average porosity of 7 percent and an average permeability of 1.6 md. The highest values are in the "C" zone where porosity averaged 12 percent and permeability 2.8 md. The average values for porosity and permeability in the "B" zone are 10 percent and 1.6 md respectively. The "A" zone is the major producing zone, but the Hamill 3-27 well is in an area of poorly developed "A" porosity. Porosities can attain 30 percent in the "A" zone, with permeabilities reaching as high as 70 md (Altschuld and Kerr, 1982).

The crossplot of core permeability and core porosity reveals some interesting relationships (Fig. 10). There is a bi-modal distribution of porosity which divides the plot into two parts: 1) the reservoir facies has porosities of eight percent or greater, and a slope of approximately 5.5. 2) The barrier or non-reservoir facies has porosities of less than eight percent, and a slope of approximately 1.5. The corresponding permeability for 8 percent porosity is

HAMILL 3-27

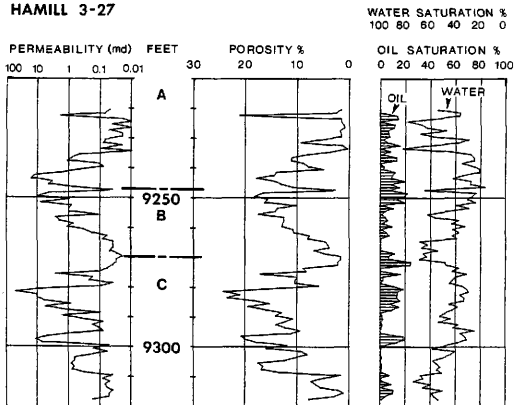


Figure 9. Porosity, permeability, and fluid saturations for the Mission Canyon reservoir section in the Hamill 3-27 core. Also shown are the "A", "B" and "C" zones.

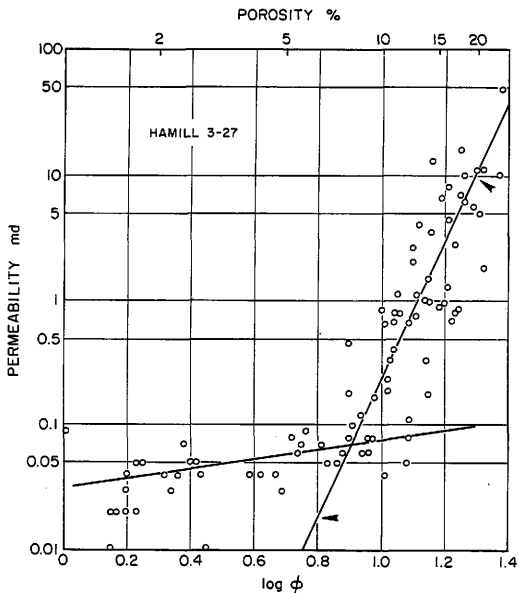


Figure 10. Cross plot of permeability and porosity from the Hamill 3-27 core (Fig. 9) showing bi-modal distribution of porosity. Also shown are average reservoir and barrier values (arrows) used in calculations (Table 7).

approximately 0.1 md; which can be considered a lower limit for adequate reservoir potential.

The "A" and "B" zones can be evaluated using the above criteria. The porosity thickness, using 8 percent as the cutoff, was mapped for both zones. The "A" zone has thicknesses in excess of 20 ft (6 m), and a large part of the field area has thicknesses greater than 15 ft (5 m) (Fig. 11). The thickness of the "B" zone rarely reaches 15 ft (5 m), and a large area is less than 10 ft (3 m) thick (Fig. 12). The "B" zone is continuous throughout the field area, while the "A" zone pinches out to the southeast. Both zones contain strike (northeast) and dip (northwest) trends, with the "A" zone trends more distinctive.

Production

The Mission Canyon Formation is a prolific reservoir in the Billings Nose area. Initial production of some of the wells was in excess of 2800 BOPD. A map of the initial production shows the quality of reservoir (Fig. 13). Production tends to mimic structure, with the greatest production occurring along the structural axis.

The majority of the production is from the "A" zone, but production has also been established in the other two zones. Whiskey Joe production is from the "B" and "C" zones, and southern TR is dominated by "B" production.

Figure 11. Net thickness of porosity greater than 8 percent in the "A" zone (Fig. 8) in the Billings Nose field area. Note porosity pinchout to the southeast. Contour interval is 5 ft (1.5 m). Circled wells mark points of control.

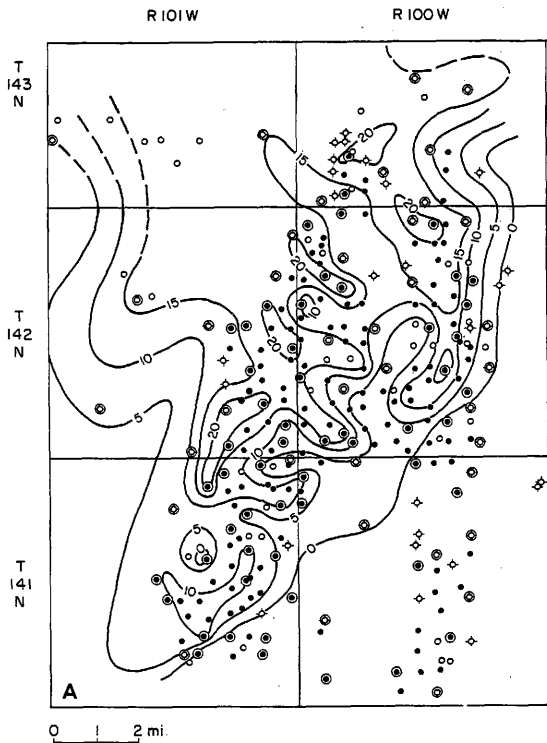


Figure 12. Net thickness of porosity greater than 8 percent in the "B" zone (Fig. 8) in the Billings Nose field area. Contour interval is 5 ft (1.5 m). Circled wells mark points of control.

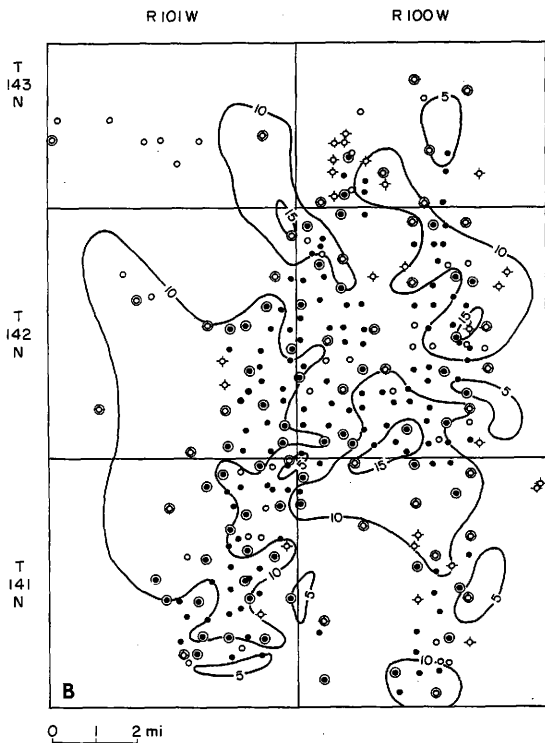
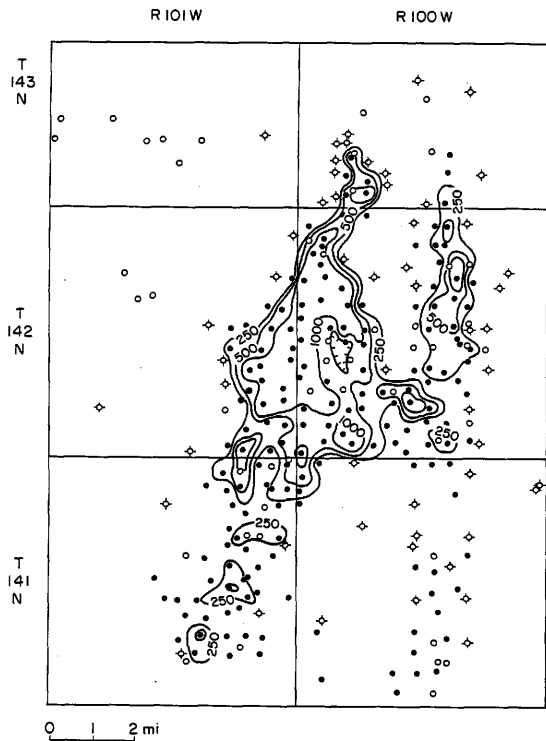


Figure 13. Initial production map for the Mission Canyon in the Billings Nose field area. Contour values in barrels of oil per day; interval varies as indicated.



There is a correlation between the percent water production (Fig. 14) and the productive zone. The areas of "B" and "C" production are marked by a higher percentage of water and lower initial production. For the most part, areas of "A" production have a lower percentage of water and higher initial production.

Nature of the Trap

Structure alone cannot explain the production in the Billings Nose area. Production occurs both on and off structure, but structure does play an important role as illustrated by the initial production map (Fig. 13). Stratigraphy also plays a vital role, with the cyclic nature of the porosity development leading to porosity pinchouts. Porous units are terminated updip by anhydrite or tight limestone. The "A" zone not only pinches out to southeast, but it also deteriorates in the southern portion of the field area.

There is a steplike pattern to the productive zones updip (depositional) in the Billings Nose region. This is illustrated in a cross-section from Rough Rider field to Fryburg field (Fig. 15). The relative stratigraphic position, both laterally and vertically, of a porous unit is important in determining its productivity. A productive unit in one area is water-wet downdip while an overlying

Figure 14. Water production map for the Mission Canyon in the Billings Nose field area showing water production as a percentage of total initial production. Contour values in percent; interval varies as indicated.

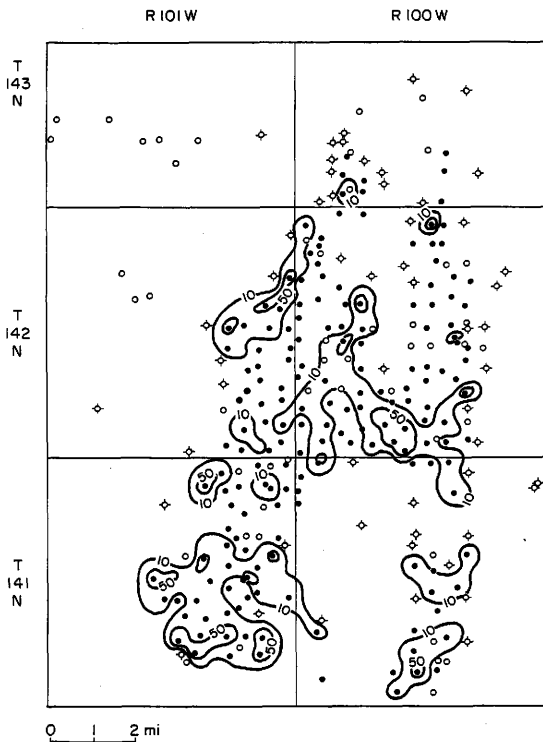
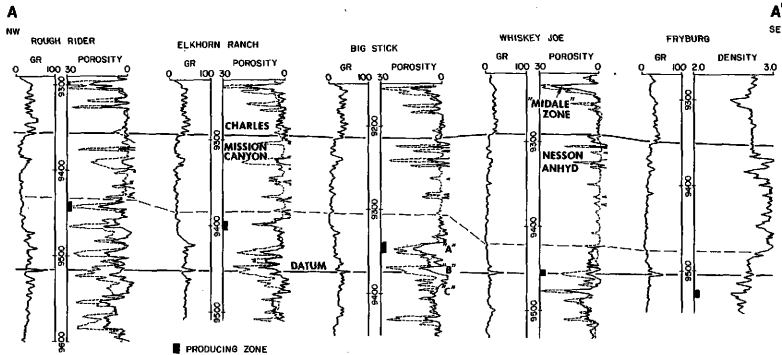


Figure 15. Regional cross section from Rough Rider field to Fryburg field showing the relationship of production to stratigraphic position of the porous zones. Also shown is the thickening of the Nesson Anhydrite to the southeast (Fig. 7). Location of cross section shown in Figure 7.



unit is oil productive.

The Billings Nose area is a combination structural and stratigraphic trap. The porous and permeable "A" zone is draped over the Billings anticline and grades laterally and updip into anhydrite or tight limestone. These same rock types provide adequate seals for the reservoir. The "B" zone production in southern TR is limited not by stratigraphic changes, but rather geographical changes. The Teddy Roosevelt National Monument lies directly to the south and no drilling has been allowed there.

HYDRODYNAMICS

Fluid Pressures

The analysis of drill-stem test (DST) pressure buildups is the basis for determining hydrodynamic flow in the Billing Nose area. Along with the essential fluid pressures, other reservoir characteristics may also be obtained from pressure buildups. The following examples show representative pressure buildups from the area.

The majority of the tests exhibit normal pressure buildups characteristic of a single reservoir. The pressure buildups from the Al-Aquitaine US 1-22 (Fig. 16) located at NE NE 22-141N-100W illustrate this condition. Extrapolation of the initial shutin (ISI) yields an original reservoir pressure (p_o) of 4377 psi, and the original reservoir pressure derived from the final shutin (FSI) is 4384 psi. Neither shutin shows any change of slope or anomalous behavior. Pressure buildups from the Shell Government 1H-20 (Fig. 17) located at SW SW 20-140N-103W show original reservoir pressures of 4301 psi and 4304 psi for the initial and final shutins, respectively.

In addition to the normal pressure buildups, there are a number of tests which exhibit anomalous buildups. An example is the FSI buildup (Fig. 18) from the Chambers

Figure 16. Pressure buildups for the initial (ISI) and final (FSI) shutin periods in the Al-Aquitaine US 1-22 showing the extrapolated original pressure (p_o). T is the total flow time and θ is the incremental shutin time.

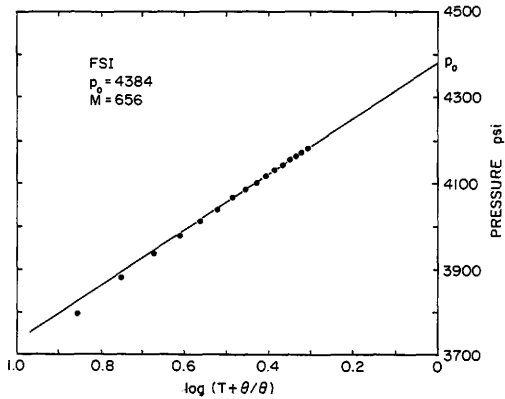
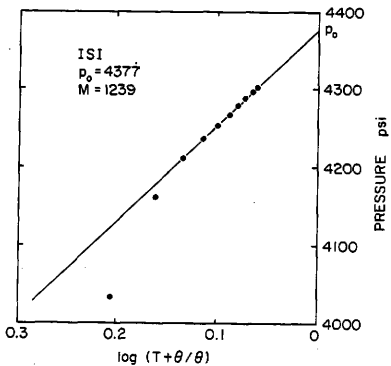
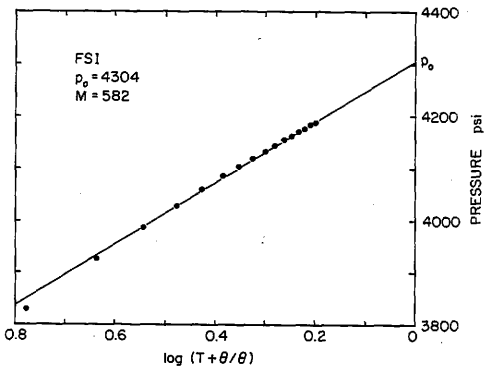
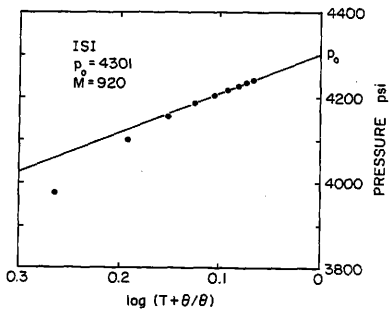


Figure 17. Pressure buildups for the initial (ISI) and final shutin (FSI) periods in the Shell Government 1H-20 showing the extrapolated original pressure (p_o).



State 1-23 located at NE NW 23-141N-101W. The character of the buildup is due to a layered reservoir with little or no communication between layers except at the borehole (Matthews and Russell, 1967). A layered character would be expected for the Mission Canyon due to the nature of the section with porous and permeable zones separated by low porosity and permeability zones. The character of the buildup is also similar to that exhibited by fracturing, although the shutin time is probably not of sufficient length to show fracturing. The FSI pressure buildup for Apache Federal 1-5 (Fig. 19) located at NE SE 5-143N-102W also exhibits a layered character, but a steady state buildup has been reached. The extrapolated original reservoir of pressure 4380 psi approximates the ISI original pressure of 4409 psi.

The extrapolation of layered buildups can lead to errors in reservoir pressures. The ISI buildup for Farmers Federal 4-33 (Fig. 20) located at NW NW 33-143N-100W, shows an original reservoir pressure of 4456 psi. This value is high due to extrapolation of the unsteady part of the final layered buildup. A better approximation for original reservoir pressure may be 4435 psi, due to the character of the previous layers.

Other anomalous buildups indicate the existence of barriers within the formation. The slope change in the FSI

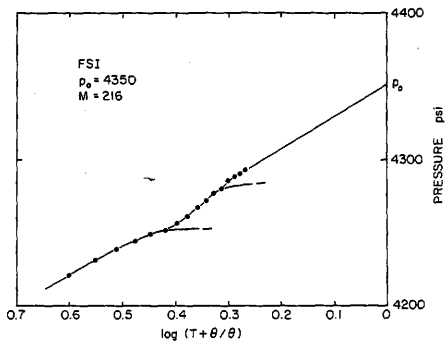


Figure 18. Pressure buildup for the final shutin (FSI) period in the Chambers State 1-23 showing layered character.

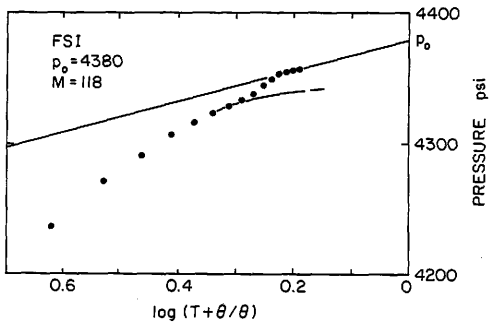


Figure 19. Pressure buildup for the final shutin (FSI) period in the Apache Federal 1-5 showing layered character and extrapolated original pressure (p_0).

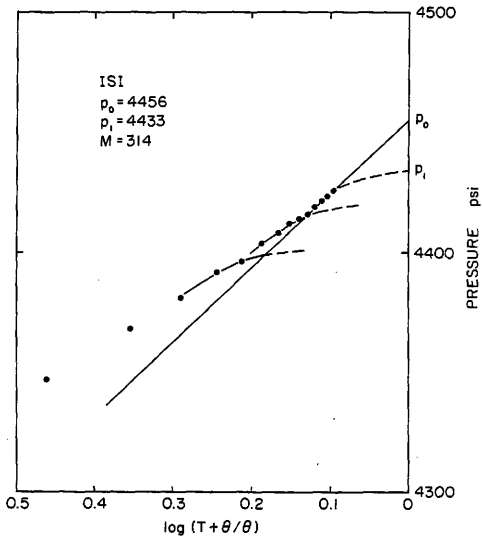


Figure 20. Pressure buildup for the initial shutin (ISI) period in the Farmers Federal 4-33 showing layered character, extrapolated original pressure (p_o) and probable original pressure (p_i).

buildup (Fig. 21) of the Patrick Federal 2-32 is indicative of a barrier. The Patrick well is located at SW NW 32-142N-100W, which is in an area of deteriorating "A" zone porosity. The decrease in permeability away from borehole is reflected in the slope change.

Potentiometric Surface

A potentiometric surface was constructed for the Billings Nose area by contouring equal freshwater hydrostatic heads. Fluid pressures were obtained from the analysis of pressure buildups from over 100 drill-stem tests in the area (Appendix B). Freshwater hydrostatic heads were calculated from fluid pressures using a constant pressure gradient of 0.433 psi/ft. This gradient was used in order to be compatible with the published potentiometric map (Fig. 2). Fluid pressures measurements in the oil column were corrected to the appropriate pressure in the water column. Only the most reliable hydrostatic heads from each township were used. The oldest tests were given preference due to amount of production in the area and possibility of pressure drawdown. Failure to reach steady state, drawdown, and excessive mud recovery were used as criteria for rejecting tests.

The regional potentiometric map (Fig. 22) for the Billings Nose area compares favorably with the published

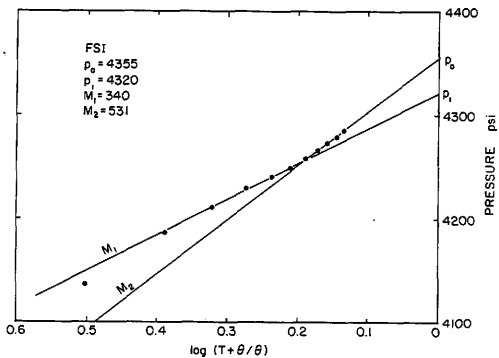


Figure 21. Pressure buildup for the final shutin (FSI) period in the Patrick Federal 2-32 showing effect of a barrier.

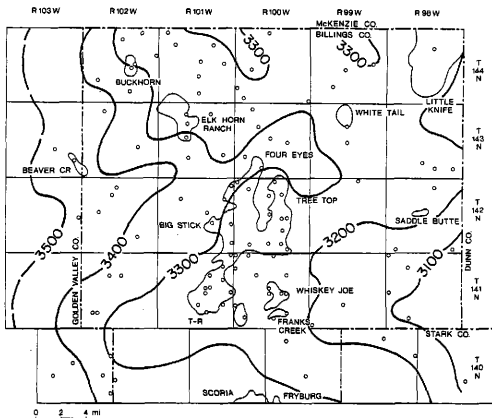


Figure 22. Regional freshwater potentiometric map for the Mission Canyon Formation. Contour interval is 100 ft (30 m). Points of control indicated in Appendix B.

potentiometric map for the Williston Basin and surrounding areas (Fig. 2). Both maps show the direction of fluid movement is generally from the west to east, and both have head values which range from 3400 to 3100 feet.

A potentiometric gradient can be established for the field area using the regional map (Fig. 22). The distance between the 3300- and the 3200-foot contours in the direction of flow across the field area is 10 miles. This establishes a gradient of 10 ft/mi, which is quite low in comparison to other gradients in hydrodynamically effected oil accumulations. It is the potential gradient, not the flow itself, which effects oil accumulations.

The validity of the potentiometric map is based on the following assumptions: 1) the Mission Canyon Formation represents a single aquifer system across the study area, and 2) the density of water remains constant over the study area. The first assumption can be supported by a plot of pressures versus elevation (Fig. 23). The elevation of the recharge area in the Black Hills is estimated at 4,500 ft which is the head at that point. The heads of the Mission Canyon, Midale and Ratcliffe, and the Bakken tests can be expressed by extending a line parallel to the 0.433 gradient to zero pressure. Flow will occur from areas of higher head to those of lower head. The Mission Canyon is a hydrodynamic system because the heads at the outcrop are

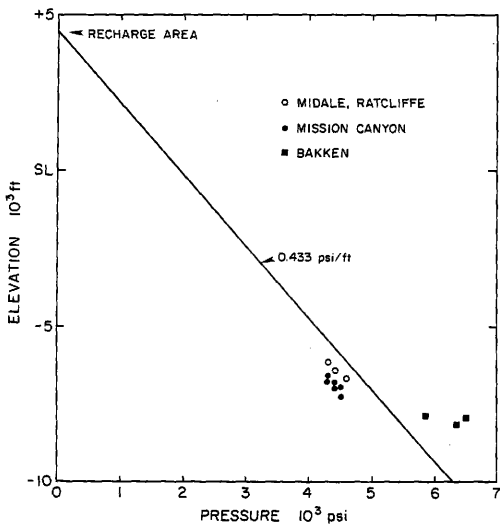


Figure 23. Plot showing pressure as a function of elevation for representative Mission Canyon, Bakken, Midale and Ratcliffe tests in the Billings Nose area.

greater than those in the field area.

The Bakken shales are overpressured due to oil generation (Meissner, 1978) and show an average gradient of 0.60 psi/ft. This gradient indicates that upward vertical flow could occur from the Bakken to the Mission Canyon. The Midale and Ratcliffe tests reveal higher heads than those in the Mission Canyon, but the impermeable Nesson Anhydrite prevents downward vertical flow into the Mission Canyon within the study area (Fig. 7).

The major factors which influence water density are temperature and salinity. The density of water increases with increasing salinity, while temperature has an inverse relationship with density. A salinity map has been published for the Williston basin (Fig. 3) and shows salinity ranging from less than 100,000 ppm to 300,000 ppm in the study area.

A regional salinity map (Fig. 24) has been constructed from drill-stem test data. The resistivities of recovered water were converted to salinities using a Schlumberger correlation chart. Only tests which recovered large quantities of water were used because of the possibility of contamination from the highly saline mud filtrate. The salinities range from less than 10,000 ppm to greater than 200,000 ppm. A lens of fresher water has invaded the Billings Nose field area from the southwest so that, within

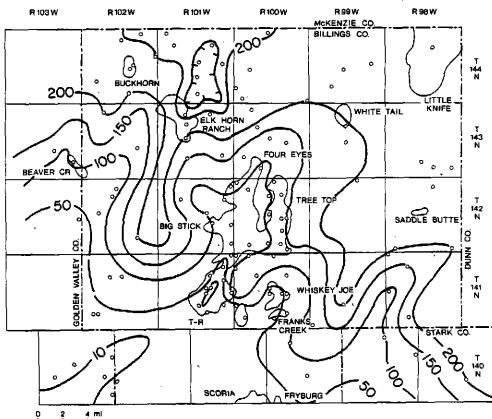


Figure 24. Regional salinity map from DST data for the Mission Canyon showing strong salinity gradient to the northeast. Contour values in parts per thousand; interval varies as indicated.

the field area, salinities range from approximately 10,000 ppm to greater than 150,000 ppm.

The assumption of a constant density for the study area is invalid due to the large salinity contrast. In a variable density system the direction and magnitude of flow may be vastly different from that portrayed by a freshwater potentiometric map.

The adjustment of the regional potentiometric map (Fig. 22) requires the correction of water densities to the existing subsurface conditions. Bottom hole temperatures (BHT) taken from drill stem tests were corrected to a depth of 9500 ft and mapped (Fig. 25). An average geothermal gradient for the area is 2° F/100 ft (MacCary, 1981), and this was used in correcting values. The central area of the map, which includes the Billings Nose field area, has temperatures greater than 240° F and in part greater than 250° F. Some of the highest temperatures in the Williston basin have been recorded in Billings County (MacCary, 1981).

Water densities were corrected to subsurface conditions using the following steps: 1) DST salinities were converted to densities at standard conditions. 2) Water-formation volume factors (Bw) were calculated for each salinity using the method outlined by Amyx, Bass and Whiting (1960). Average temperature and pressure were

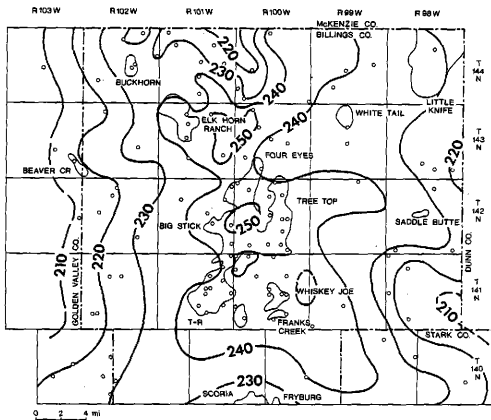


Figure 25. Regional temperature map from DST data. Corrected to -9500 ft (-2896 m) using geothermal gradient of 2° F/100 ft (40° C/km). Contour interval is 10° F.

assumed to be 240° F and 4300 psi respectively. 3) Subsurfaces densities were calculated using the standard density and water-formation volume factor. The proper pressure gradient was calculated for each subsurface density. The results of the calculations are displayed in Table 3.

A revised potentiometric map (Fig. 26) was constructed using the regional salinity map (Fig. 24) in conjunction with the proper pressure gradients. Corrections in the pressure gradient were made using a constant density for each salinity interval as shown in Table 4. The contrast between the freshwater potentiometric map (Fig. 22) and the revised map (Fig. 26) is striking. The original map has a low gradient of 10 ft/mi and flow from west to east, while the revised map shows flow generally southwest to northeast at a much higher gradient of 50 ft/mi. The magnitude of the fluid density corrections are such that the revised map resembles the regional salinity map (Fig. 24), with flow in the direction of increasing salinity. The fresher water lens which invades the Billings Nose field area from the southwest has changed the gradient across the field from 10 ft/mi to 50 ft/mi. The direction of flow has also changed from generally easterly, which is across structure to northeasterly and downdip.

Pickett plots or resistivity versus porosity plots

Table 3. Conversion of salinities to pressure gradients.

Salinity (ppm)	Surface Density (g/cm ³)	Subsurface Density (g/cm ³)	Pressure Gradient (psi/ft)
50,000	1.037	1.000	0.433
100,000	1.071	1.028	0.445
150,000	1.104	1.061	0.459
200,000	1.134	1.095	0.474

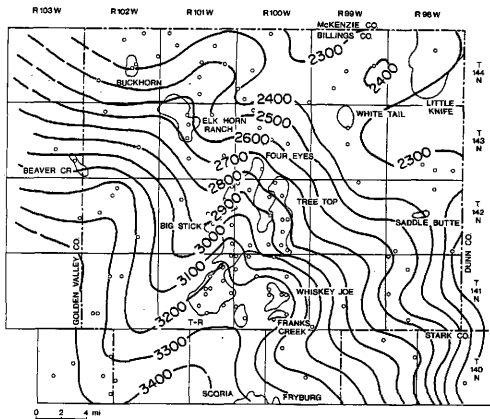


Figure 26. Regional corrected potentiometric map showing strong gradient to the northeast. Corrected using regional salinity map (Fig. 24) in conjunction with Tables 3 and 4. Contour interval is 100 ft (30 m).

Table 4. Values used in correction of potentiometric maps.

Interval (ppm)	Pressure Gradient (psi/ft)
< 50,000	0.433
50,000-100,000	0.440
100,000-150,000	0.452
150,000-200,000	0.468
> 200,000	0.474

were constructed for wells in the field area to determine water resistivities. There is a change from high water resistivities in the southern part of the field to low water resistivities in the north. The following examples are representative of the change. The plot (Fig. 27) for the Patrick Hamill 3-27 well located SW NE 27-14N-101W revealed a water resistivity of 0.09 ohm-m. An intermediate resistivity of 0.054 ohm-m was obtained from the Tenneco 3-25 well (Fig. 28) located at SW SW 25-142N-101W. In contrast, a water resistivity of 0.018 ohm-m was obtained from the Tenneco Stuart 3-7 well (Fig. 29) located at SW NE 7-142N-100W. The calculated resistivities were confirmed by water resistivity measurements from DSTs in nearby wells.

A map of the water resistivities (Fig. 30) reveals a lens of higher resistivity water extending into the field area from the southwest. The location of the lens appears to be structurally controlled in that the higher resistivity water extends downdip along the crest of the anticline.

The water resistivities were converted to salinities assuming an average temperature of 240° F (Table 5). The resulting salinity map (Fig. 31) is similar to the regional salinity map (Fig. 24) derived from drill-stem test data. The salinities in the field area range from

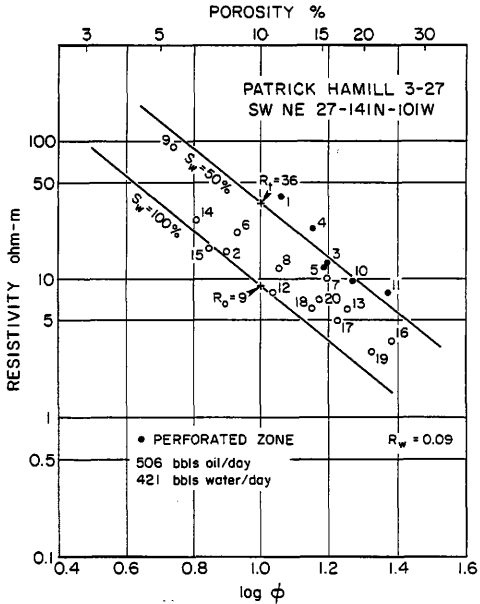


Figure 27. Pickett plot for Patrick Hamill 3-27 showing water resistivity (R_w) of 0.09 ohm-m and variations in water saturation (S_w).

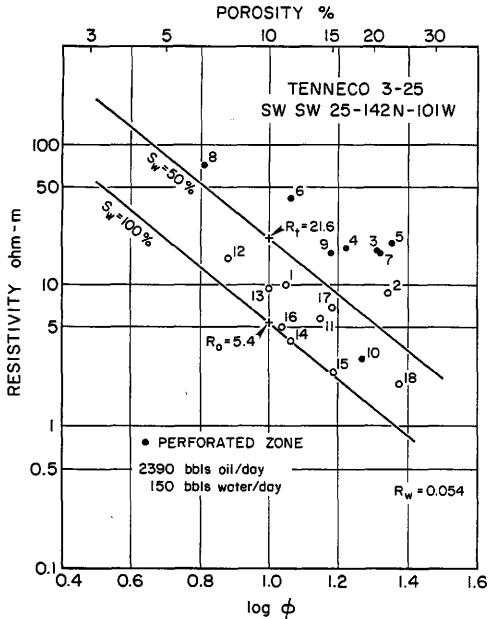


Figure 28. Pickett plot for Tenneco 3-25 showing water resistivity (R_w) of 0.054 ohm-m and variations in water saturation (S_w).

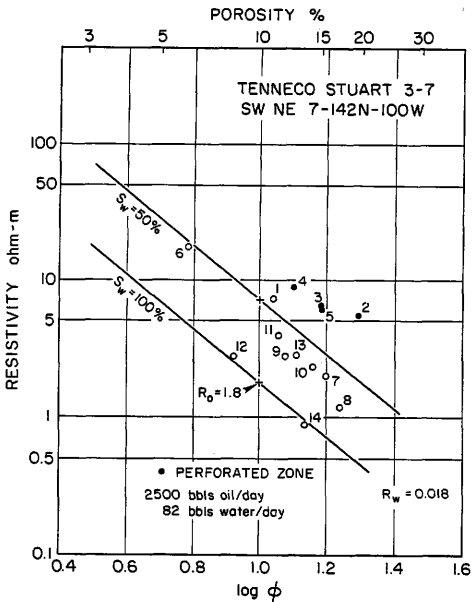


Figure 29. Pickett plot for Tenneco Stuart 3-7 showing water resistivity (R_w) of 0.018 ohm-m and variations in water saturation (S_w).

Figure 30. Water resistivity map from log interpretation (Figs. 27, 28, 29) in the Billings Nose field area showing location of high resistivity lens. Contour interval 0.01 ohm-meters.

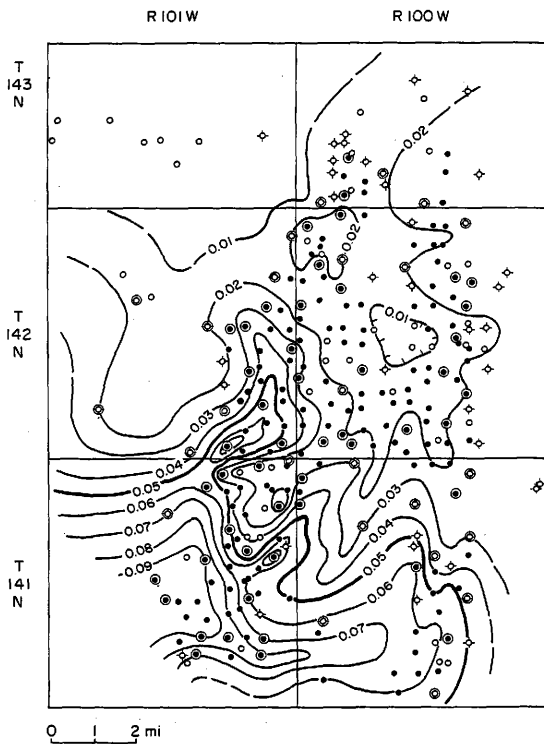


Table 5. Conversion of water resistivities to salinities.

Water Resistivity @ 240° F ohm-meters	Salinity ppm
0.09	22,000
0.08	25,000
0.07	29,000
0.06	35,000
0.05	44,000
0.04	57,000
0.03	80,000
0.02	135,000
0.015	200,000
0.01	200,000+

approximately 20,000 ppm in the southwestern section to greater than 200,000 ppm in the northern area. A field potentiometric map (Fig. 32) was constructed using the field salinity map to correct fluid densities as set forth in Table 4.

The map shows that fluid movement is generally to the northeast across the field area at a high gradient. The potentiometric gradient can be established using average values from Figure 32. The distance between the 3300 ft contour which lies updip, and the downdip 2500 ft contour is 16 miles. These values establish a gradient of 50 ft/mi across the field. In contrast, the freshwater field potentiometric map (Fig. 33) yields a gradient of only 10 ft/mi in a generally easterly direction.

Interpretation

The differences between the freshwater potentiometric map and the corrected field potentiometric map are due to the large salinity contrast across the field. Possible errors in fluid pressure measurements are negligible in comparison to the hydrostatic head differences caused by varying salinities. If the assumptions of a fluid pressure of 4300 psi, temperature of 240^o F, and no change in subsurface elevations are made, then a difference of approximately 600 feet of head would result from a change

Figure 31. Billings Nose field area salinity map from water resistivity values (Fig. 30). Contour values in parts per thousand; interval varies as indicated.

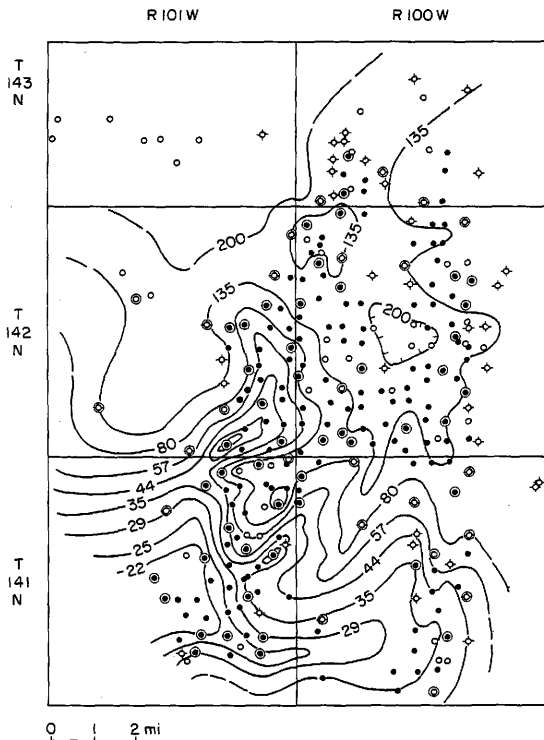


Figure 32. Corrected Billings Nose field area potentiometric map showing strong gradient to the northeast. Corrected using field salinity map (Fig. 31) in conjunction with Table 4. Contour interval 100 ft (30 m).

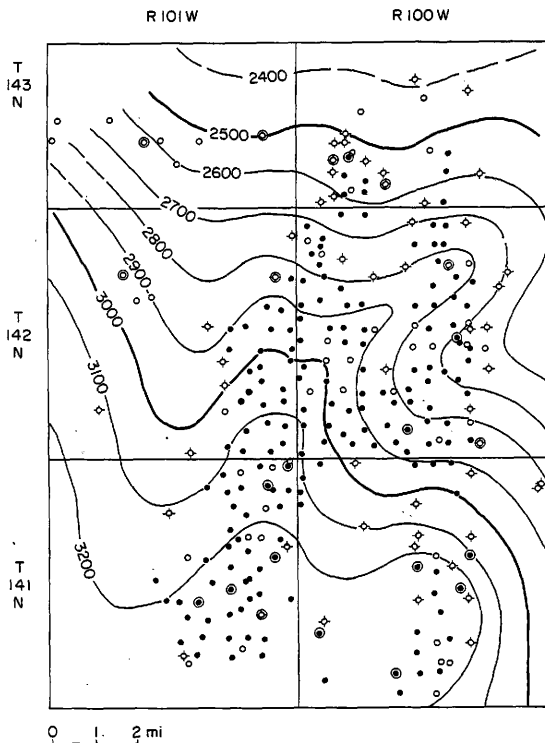
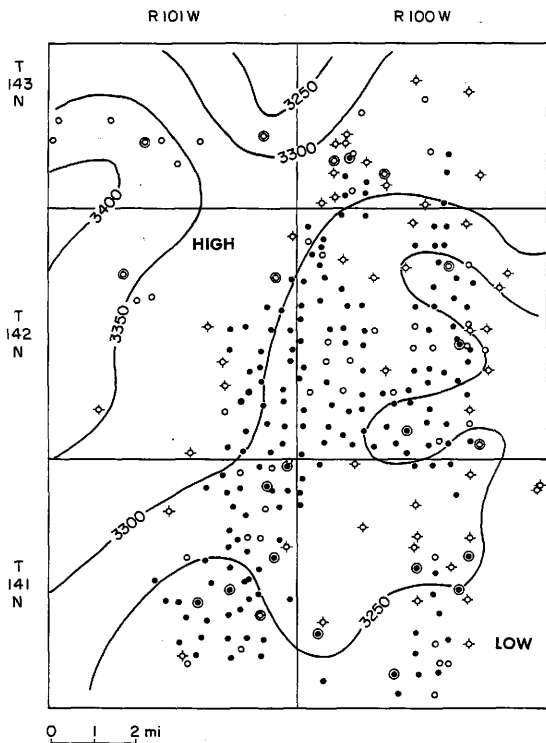


Figure 33. Billings Nose field area freshwater
potentiometric map. Contour interval 50 ft. (15 m).
Circled wells indicate points of control.



of salinity from less than 50,000 ppm to greater than 150,000 ppm. This is the type of salinity contrast which occurs across the field area as confirmed by both the DST salinity map and the water resistivity map from log interpretations. A water production salinity map from Tenneco (B. Desidier, 1985, pers. comm.) reveals a similar salinity contrast across the field.

There are differences between the Tenneco salinity map and the salinity map derived from log interpretation. The water from which Tenneco obtained salinity values originated from the "A" and "B" porosity zones as water produced with oil. On the other hand, the water resistivities from log interpretation were taken from the underlying "C" zone. This difference implies that while the overall salinity contrast is the same, a vertical contrast also exists as illustrated in the diagrammatic cross-section (Fig. 34). The "C" zone has the highest average porosities and permeabilities in the southwestern section as shown in the Hamill 3-27 core. The "C" zone would be structurally higher as well as more continuous to the south in comparison to the "A" and "B" zones. Therefore, the "C" zone is more deeply invaded by the fresher waters. A vertical salinity gradient can be documented from DST recoveries and confirms the vertical change illustrated in the cross section (Fig. 34).

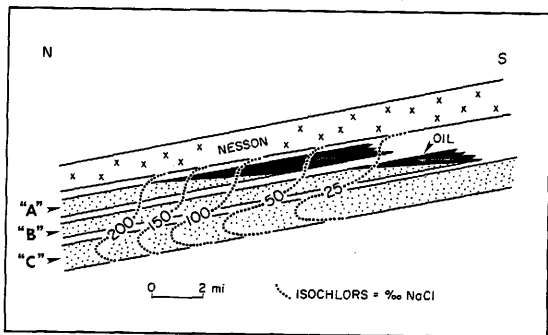


Figure 34. Diagrammatic cross section in Billings Nose field area showing water salinity change in relation to porosity zones.

OIL ACCUMULATION

Oil Source

The source rock for the Mission Canyon reservoirs in the Billings Nose area, as well as the rest of the basin, is the Bakken Formation. Williams (1974) presented geochemical evidence based on carbon isotope ratios that the Bakken was the source rock for the Madison oils. Thode (1981) came to a similar conclusion based on similarities in sulfur isotopes.

The Bakken Formation is organic-rich, with organic carbon content ranging from 5 to 20 percent by weight (Webster, 1984). The average in the Billings Nose area is approximately 10 percent by weight. A minimum value of one percent organic carbon has been proposed for evaluating source rocks (Merewether and Claypool, 1980). On the basis of geochemical evidence, such as vitrinite reflectance, pyrolysis, and extracted hydrocarbons, Webster (1984) concluded that the Bakken shale within the study area has reached a state of intense oil generation.

The maturation of a source rock is time and temperature dependent. A temperature increase has the same effect as increasing the source rock exposure time at a lower temperature. Waples (1980) has demonstrated that the timing of oil generation can be predicted by applying these

principles to a burial history of the source rock. The burial history of the Bakken shale in the field area has been constructed (Fig. 35). This is essentially the same diagram as presented by Webster (1984) except the burial depth has been adjusted and a geothermal gradient of 2.2° F/100 ft (40° C/km) was used. The higher geothermal gradient was taken from MacCary (1981) and corresponds to the gradient in the Billings Nose field area.

Time and temperature calculations were made from Figure 35 by estimating the time the Bakken spent in each temperature interval of 10° C. This time was then multiplied by a temperature factor to obtain a time-temperature index (TTI). The total TTI was calculated by summing the TTI values for each interval. The calculations were made using the Waples (1980) method and are displayed in Table 6.

The onset of oil generation occurs when the total TTI value reaches 15 (Waples, 1980). This occurred approximately 80 million years ago in Late Cretaceous time when the Bakken reached a depth in excess of 8,500 feet (2591 m). According to Waples (1980) oil generation ceases when the total TTI reaches 160, and using this criterion the Bakken should be a spent source. This conclusion is contradicted by existing geochemical evidence and the fact that some wells in the area produce oil from the Bakken.

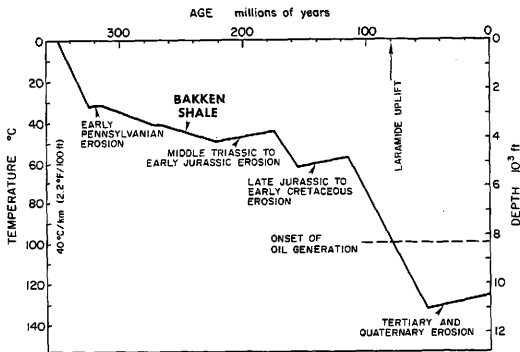


Figure 35. Lopatin diagram for the Bakken Shale in the Billings Nose area showing burial history and onset of oil generation. Modified from Webster (1984).

Table 6. Calculation of time-temperature index (TTI) for burial history of Bakken Shale in Figure 35.

Temp. Interval	Temp. Factor	Time (m.y.)	Interval TTI	Total TTT
30 - 40°C	2^{-7}	50	0.39	0.39
40 - 50	2^{-6}	107	1.67	2.06
50 - 60	2^{-5}	41	1.28	3.34
60 - 70	2^{-4}	24	1.50	4.84
70 - 80	2^{-3}	8	1.00	5.84
80 - 90	2^{-2}	8	2.00	7.84
90 - 100	2^{-1}	8	4.00	11.84
100 - 110	1	8	8.00	19.84
110 - 120	2	8	16.00	35.84
120 - 130	4	48	192.00	227.84
130 - 140	8	12	96.00	323.84

The discrepancy probably results from applying the present geothermal gradient as a constant through geologic time.

Oil Migration

The primary migration of oil from the Bakken probably occurred in continuous-phase in response to differential pressures. Dow (1974) presented a model for migration of Bakken oil, in which the oil migrated upward through vertical fractures associated with anticlinal axes into the overlying Lodgepole Formation. Vertical migration continued into the Mission Canyon Formation but was impeded when the Charles salt was encountered. After reaching the impermeable salt, migration continued laterally updip beneath the salt within the porous units of the Mission Canyon until structurally or stratigraphically trapped. Meissner (1978) has proposed that the vertical fracture paths are extensive, not just associated with structures and are induced by fluid overpressuring. The abnormal fluid pressures result from hydrocarbon generation. Fluid pressures of between 0.60 and 0.80 psi/ft would be required to open fractures. Once the fractures are opened the hydrocarbons would migrate, thus reducing pressure and sealing the fracture until more hydrocarbons were produced.

The Billings Nose area lies in a region of active oil generation and thus fluid overpressuring. The average

fluid pressure gradient of the Bakken tests shown in Figure 23 is 0.60 psi/ft. Flow would occur upwards into the Lodgepole and then the Mission Canyon. The Nesson Anhydrite would impede the vertical migration and cause lateral updip migration. This explains the importance of the highest porous zone beneath the Nesson in relation to production as shown in the regional cross section (Fig. 15).

Oil Column Calculations

The oil accumulation in the Billings Nose appears to be a combination structural and stratigraphic trap. The pinchout of the porous and permeable "A" zone is superimposed on the broad, gently plunging anticlinal structure. Downdip hydrodynamic flow also occurs in the field area and should have a strong influence on the oil column. The productive limits of the field in conjunction with structure contours can be used to estimate the total oil column of approximately 150 ft. Oil column calculations can be made using available data on rock properties and fluid pressures.

Capillary Oil Column

The hydrostatic oil column trapped by capillary pressure differences is based on the contrasts in porosity

and permeability of the reservoir and barrier facies (Berg, 1975). Using the equations presented by Berg (1972, 1975), equation (4) and the data from Table 7, the hydrostatic oil column can be calculated.

Capillary pressure trapping accounts for only 24 ft of the total oil column of 150 ft in the Billings Nose field. In order to apply the equations, the reservoir values of porosity and permeability were taken from the higher part of the plot of porosity versus permeability from the Hamill 3-27 well (Fig. 10). The barrier porosity and permeability values were taken from the lowest part of the plot corresponding to the reservoir facies (Fig. 8). The actual barrier facies probably has similiar permeability but is less porous. For this reason the oil column calculation should be viewed as a minimum.

Hydrodynamic Oil Column

Berg (1975) has shown that downdip hydrodynamic flow can account for a substantial amount of additional oil column. The hydrodynamic oil column can be calculated using equation (5). The potentiometric gradient is approximately 50 ft/mi in the downdip direction. The horizontal width of oil accumulation is approximately 12 miles in the direction of dip. The subsurface oil and water densities are 0.625 g/cm^3 and 1.028 g/cm^3 ,

Table 7. Summary of oil column calculations and rock and fluid properties for the Mission Canyon Formation.

	Reservoir	Barrier
Porosity, %	20	6
Permeability, md	10	0.02
Effective Grain Size, cm	2.09×10^{-3}	2.02×10^{-3}
Pore Radius, cm	4.33×10^{-4}	----
Pore Throat Radius, cm	----	1.55×10^{-4}
Capillary Oil Column, ft		24
Hydrodynamic Oil Column, ft		1530
Total Oil Column, ft (calculated)		1554
Observed Oil Column, ft		150
Oil Gravity, $^{\circ}\text{API}$		40
Surface Oil Density (D_o)		0.825
Gas/Oil Ratio, ft^3/bbl		900
Gas Density		0.7 (assumed)
Water Salinity, ppm	100,000 (average)	
Water Surface Density (D_w)		1.071
Temperature, $^{\circ}\text{F}$		240
Pressure, psi		4300
Interfacial Tension, dynes/cm^3		35
Oil Formation Volume Factor (B_o)		1.54
Subsurface Oil Density (D_o)		0.625
Subsurface Water Density (D_w)		1.028

respectively, assuming a salinity of 100,000 ppm. The amplification factor is 2.55.

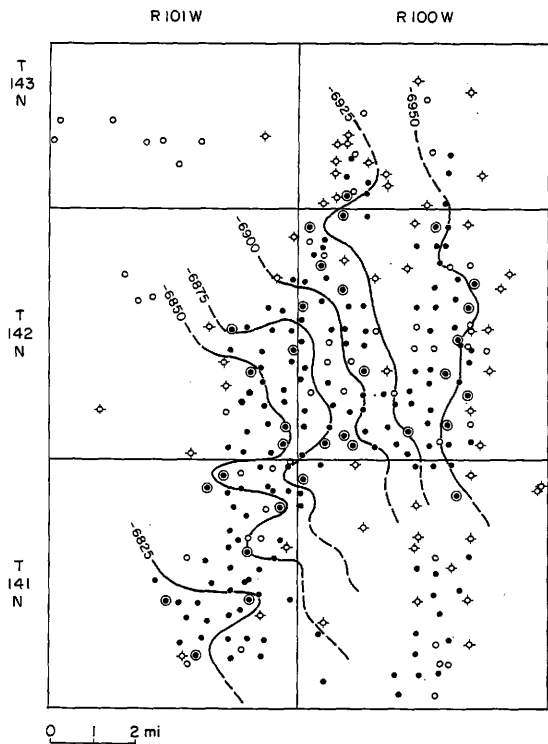
The calculated hydrodynamic oil column is 1530 ft, which is approximately 10 times greater than the observed oil column. It is apparent that the oil accumulation is not in equilibrium with the hydrodynamic gradient estimated for the area.

Oil-Water Contact

The oil-water contact will be tilted in areas of hydrodynamic flow (Hubbert, 1953) and the magnitude of tilt can be calculated using equation (3). The potentiometric gradient is approximately 50 ft/mi and the amplification factor is 2.55. The calculated tilt of the oil-water contact is approximately 127.5 ft/mi in a northeasterly direction. This far exceeds the structural dip in the area and implies that flushing of the oil should have occurred or is occurring now.

An apparent oil-water contact map (Fig. 36) was constructed from completion card information and the highest occurrence of water on the Pickett plots (Figs. 27, 28, 29). The tilt of the oil-water contact is approximately 25 ft/mi in a generally northeasterly direction. This is 5 times less than the calculated tilt and implies that the oil accumulation is not in equilibrium

Figure 36. Apparent oil-water contact map for the Billings Nose field showing gentle tilt to the northeast. Contour interval is 25 ft (8 m). Circled wells indicate points of control.



with the existing potentiometric gradient, but is in a state of transition.

History of Oil Accumulation

The total oil column, tilt of the oil-water contact and the existence of the oil accumulation itself are in opposition to the expected effects of the strong potentiometric gradient in the area. A better understanding of the problem can be achieved through a chronological reconstruction of events affecting the oil accumulation.

The onset of oil generation in the Bakken began approximately 80 million years ago in Late Cretaceous time (Fig. 35). According to existing geochemical evidence, oil generation is still taking place. The timing of primary migration is uncertain, but may have begun between 70 and 75 million years ago and may still be occurring. The initial trapping of oil probably occurred shortly after initial migration.

The Laramide orogeny began during the Late Cretaceous (80 million years ago) and continued through the Early Eocene (52 million years ago). The most active period was during the Paleocene and Early Eocene. The present structural configuration of the Billings Nose area is a result of deformation during the orogeny, but the exact

timing is uncertain. Since the Paleocene was the time of peak orogenic activity, the deformation may have occurred then, approximately 60 million years ago. The deformation may also have created some fracturing which would have enhanced primary and secondary migration. The orogeny also uplifted the Black Hills region and exposed the Paleozoic and Cretaceous rocks to erosion. The erosion probably occurred not earlier than Early Eocene (52 my ago) and not younger than Oligocene (37 my ago).

The initial accumulation of oil in the Billings Nose area probably occurred under essentially hydrostatic conditions. This is a safe assumption because the present hydrodynamic regime would have prevented the accumulation. The extent of the accumulation was probably similar to that illustrated in Fig. 37 (A).

The exposure and recharge of the Mission Canyon Formation would have initiated hydrodynamic conditions within the basin. At this time the Billings Nose area may have been a region of constant salinity, probably in excess of 100,000 ppm. The actual salinity value would not be as important as assuming that it was constant throughout the region. If a constant density is assumed, then the freshwater potentiometric map (Fig. 22) is representative of the hydrodynamic conditions at that time. The difference between the actual subsurface density and

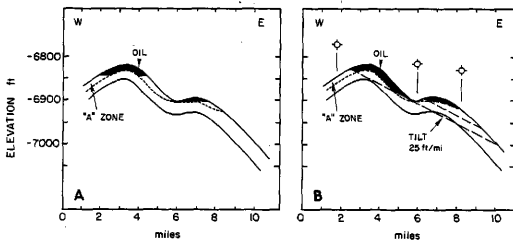


Figure 37. Diagrammatic cross section through center of Billings Nose field area showing oil accumulation under hydrostatic conditions (A) and hydrodynamic conditions (B). Vertical exaggeration is 125 times.

density used in construction of the map would have had little effect on the potentiometric gradient. The actual head values would be different but the gradient would remain essentially the same.

The potentiometric gradient established from Figure 22 is approximately 10 ft/mi to the east. The tilt amplification factor is 2.55 or less depending on the actual water density. The resultant tilt of the oil-water contact under these conditions would be approximately 25 ft/mi to the east. The apparent tilt of the present accumulation as obtained from Figure 35 is approximately 25 ft/mi to the northeast. This implies that the accumulation was subjected to hydrodynamic conditions similar to those depicted by the freshwater potentiometric map. The configuration of the oil accumulation under these conditions is illustrated in Figure 36 (B) and is similar to the present accumulation.

If the present hydrodynamic conditions had been in effect a sufficient length of time, then the oil accumulation would have been flushed from the Billings Nose area. This implies that the freshwater lens and its accompanying hydrodynamic effects are just now reaching the field area. The oil accumulation is in the process of reaching a state of equilibrium with the hydrodynamic conditions. The water production map (Fig. 14) shows the

areas of water-free oil rimmed by water production on the eastern side of structure. The regions of lower salinity also have the higher percentage of water production. Thus, it appears that the present hydrodynamic flow is tilting the oil accumulation and is in the process of flushing the structure.

The rate of movement can be calculated for the freshwater lens, if it is assumed that the lens has recently reached the Billings Nose area. The distance to the recharge area in the Black Hills is approximately 175 miles. The second phase of recharge of the Mission Canyon is assumed to have occurred approximately 2 million years ago after the last stage of vulcanism in the Black Hills, which makes the rate of movement of the lens only 0.46 ft/year. At this rate the Billings Nose area could be flushed in approximately 135,000 years.

CONCLUSION

The Mission Canyon oil accumulations in the Billings Nose area are not in equilibrium with the present hydrodynamic conditions. The oil accumulations will eventually be flushed from the area under the existing hydrodynamic regime. This conclusion implies that at the time of entrapment the hydrodynamic conditions were different.

Extrapolation of pressure buildups from drill-stem tests were used to construct a regional freshwater potentiometric map. This map indicates that flow is generally west to east and the hydrodynamic gradient across the field area is approximately 10 ft/mi. A corrected potentiometric map was constructed to account for with the variations in fluid density. The estimated hydrodynamic gradient across the field from this map is approximately 50 ft/mi in a generally northeasterly direction. The differences in the two maps are due to the salinity contrast across the field. This salinity contrast is largely due to a fresher water lens which has invaded the field from the southwest. The existence of this lens was confirmed by a field salinity map derived from well log interpretations by resistivity versus porosity crossplots.

The calculated total oil column, tilt of the oil-water contact and the location of the oil accumulation itself

imply that the oil accumulation is not in equilibrium with the present hydrodynamic gradient. The initial entrapment probably took place under hydrostatic conditions, and this period was followed by hydrodynamic and constant density conditions similiar to those depicted by the freshwater potentiometric map. The present hydrodynamic conditions are caused by the fresher water lens which has recently moved into the field area and with sufficient time will flush the area of oil.

The use of drill-stem test data to understand the hydrodynamic regime of an area is important in oil and gas exploration and development. The strong effect that salinity variations have on a hydrodynamic system is important when exploring in areas of varying salinity. The value of well log interpretation to determine water resistivities, and thus improve log interpretation, has been demonstrated. Future exploration this trend should integrate fluid-pressure and salinity data along with the structural and stratigraphic data for the best results.

REFERENCES CITED

- Altschuld, N., and S.D. Kerr, Jr., 1982, Mission Canyon and Duperow reservoirs of the Billings Nose, Billings County, North Dakota: 4th International Williston Basin Symposium, Regina, Saskatchewan, p. 103-112.
- Amyx, J.W., D.M. Bass, and R.L. Whiting, 1960, Petroleum Reservoir Engineering, New York, McGraw-Hill, 610 p.
- Berg, R.R., 1972, Oil column calculations in stratigraphic traps: Transactions of the Gulf Coast Association of Geological Societies, v. 22, p. 63-66.
- _____, 1975, Capillary Pressures in Stratigraphic Traps: American Association of Petroleum Geologists Bulletin, v. 59, p.939-956.
- _____, 1976, Trapping mechanisms for oil in Lower Cretaceous Muddy sandstone at Recluse Field, Wyoming: Wyoming Geological Association Guidebook--Twenty-Eighth Annual Field Conference, p. 261-272.
- Bjorlie, P.F., and S.B. Anderson, 1978, Stratigraphy and depositional setting of the Carrington Shale facies (Mississippian) of the Williston basin, in The economic geology of the Williston basin: Williston Basin Symposium, Montana Geol. Soc., p. 165-177.
- Bridges, L.W.D., 1978, Red Wing Creek field, North Dakota: a concentricline of structural origin, in The economic geology of the Williston basin: Williston Basin Symposium, Montana Geol. Soc., p. 315-326
- Brown, D.L., 1978, Wrench-style deformational patterns associated with a meridional stress axis recognized in Paleozoic rocks in parts of Montana, South Dakota, and Wyoming, in The economic geology of the Williston basin: Williston Basin Symposium, Montana Geol. Soc., p. 17-35.
- Carlson, C.G., and S.B. Anderson, 1965, Sedimentary and tectonic history of North Dakota part of Williston basin: American Association of Petroleum Geologists Bulletin, v. 49, p. 1833-1846.

- Carroll, W.K., 1978, Depositional and paragenetic controls on porosity development, Upper Red River Formation, North Dakota, in The economic geology of the Williston basin: Williston Basin Symposium, Montana Geol. Soc., p. 79-94.
- Darcy, H., 1856, Les fontaines publiques de la ville Dijon, Victor Dalmont, Paris.
- Dow, W.G., 1974, Application of oil correlation and source-rock data to exploration in Williston basin: American Association of Petroleum Geologists Bulletin, v. 58, p. 1253-1262.
- Downey, J.S., 1984, Geology and hydrology of the Madison limestone and associated rocks in parts of Montana, Nebraska, North Dakota, South Dakota, and Wyoming. U.S. Geological Survey Professional Paper 1273-G, 152 p.
- Edie, R.W., 1958, Mississippian sedimentation and oil fields in southeastern Saskatchewan: American Association of Petroleum Geologists Bulletin, v. 42, p. 94-1126.
- Fish, A.R., and J.C. Kinard, 1959, Madison Group stratigraphy and nomenclature in the northern Williston basin: American Association of Petroleum Geologists Geologic Record, Rocky Mountain Section, p. 117-130.
- Foster, N.H., 1972, Ordovician System, in Geologic Atlas of the Rocky Mountain region, U. S. A.: Rocky Mountain Assoc. Geologists, p. 76-86.
- Freeze, R.A., and J.A. Cherry, 1979, Groundwater, Englewood Cliffs, N. J., Prentice-Hall, 604 p.
- Fuller, J.G.C.M., 1956, Mississippian rocks in Saskatchewan portion of the Williston basin: First International Williston Basin Symposium, p. 29-35.
- Gerhard, L.C., S.B. Anderson, J.A. Lefever, and C.G. Carlson, 1982, Geological development, origin, and energy mineral resources of Williston basin, North Dakota: American Association of Petroleum Geologists Bulletin, v. 66, p. 989-1020.

- Hamke, J.R., L.C. Marchant, and C.Q. Cupps, 1966, Oil-fields in the Williston basin in Montana, North Dakota, and South Dakota: U.S. Bureau of Mines Bull. 629, 134 p.
- Hansen, A.R., 1972, Economic geology of the Williston basin, in Geologic Atlas of the Rocky Mountain region, U. S. A.: Rocky Mountain Assoc. Geologists, p. 329-334.
- Hack, T., 1978, Depositional environments of the Bottineau interval (Lodgepole) in North Dakota, in The economic geology of the Williston basin: Williston Basin Symposium, Montana Geol. Soc., p. 191-203.
- Horner, D.R., 1951, Pressure build-up in wells: Third World Petroleum Congress Proceedings, Leiden, Section 2, p. 503-523.
- Hubbert, M.K., 1940, Theory of ground water motion: Journal of Geology, v. 48, p. 785-944.
- _____, 1953, Entrapment of petroleum under hydrodynamic conditions: American Association of Petroleum Geologists, v. 37, p. 1954-2026.
- Kupez, J.A., 1984, Depositional environments, diagenetic history, and petroleum entrapment in the Mississippian Frobisher-Alida interval, Billings anticline, North Dakota: Colorado School of Mines Quarterly, v. 79, no. 3, 53 p.
- Larberg, G.M., 1976, Hydrodynamic effects on oil accumulation in a stratigraphic trap, Kitty Field, Powder River basin, Wyoming, Unpublished M.S. thesis, Texas A&M Univ., 180 p.
- Levorsen, A.I., and F.A.F. Berry, 1967, Geology of Petroleum, 2nd ed., San Francisco, W.H. Freeman, 724 p.
- Lin, J.T.C., 1981, Hydrodynamic flow in Lower Cretaceous Muddy Sandstone, Gas Draw Field, Powder River basin, Wyoming: Mountain Geologist, v. 18, no. 4, p. 78-87.
- Lindsay, R.F., and M.S. Roth, 1982, Carbonate and evaporite facies, diagenesis and reservoir distribution of the Mission Canyon Formation, Little Knife Field: Fourth International Williston Basin Symposium, Regina, Saskatchewan, p. 153-179.

- Lindsey, K.B., 1954, Petroleum in the Williston basin, including parts of Montana, North and South Dakota, and Canada, as of July, 1953: U.S. Bureau of Mines Report of Investigations 5055, 88 p.
- Lochman-Balk, C., 1972, Cambrian System, in Geologic Atlas of the Rocky Mountain region, U. S. A.: Rocky Mountain Assoc. Geologists, p. 60-76.
- MacCary, L.M., 1981, Apparent resistivity, porosity, and ground-water temperature of the Madison limestone and underlying rocks in parts of Montana, Nebraska, North Dakota, South Dakota, and Wyoming, USGS Open-File Report 81-629, 40 p.
- Matthews, C.S., and D.G. Russell, 1967, Pressure buildup and flow tests in wells, Society of Petroleum Engineers of AIME, Monograph Volume 1, 167 p.
- Meissner, F.F., 1978, Petroleum geology of the Bakken Formation, Williston basin, North Dakota and Montana, in The economic geology of the Williston basin: Williston Basin Symposium, Montana Geol. Soc., p. 207-227.
- Merewether, E.A., and G.E. Claypool, 1980, Organic composition of some Upper Cretaceous shale, Powder River basin, Wyoming: American Association of Petroleum Geologists Bulletin, v. 64, p. 488-500.
- Miller, W.R., and S.A. Strausz, 1980, Preliminary map showing freshwater heads for the Mission Canyon and Lodgepole limestones and equivalent rocks of Mississippian Age in the northern Great Plains of Montana, North and South Dakota, and Wyoming, USGS Open-File Map 80-729 (Water-Resources Investigations).
- Munn, M.J., 1909, The anticlinal and hydraulic theories of oil and gas accumulation: Econ. Geology, v. 4 p. 509-529.
- Murray, G.H., 1959, Examples of hydrodynamics in the Williston basin at Poplar and North Tioga fields: American Association of Petroleum Geologists, Geological Record, Rocky Mountain Section, p. 55-60.
- Pickett, G.R., 1966, A review of current techniques for determination of water saturation from logs: Journal Petroleum Technology, v. 18, p. 1425-33.

- Proctor, R.M., and G. Macauley, 1956, Mississippian of western Canada and Williston basin: American Association of Petroleum Geologists Bulletin, v. 52, p. 1956-1968.
- Rygh, M.E., 1983, Production performance curves of selected North Dakota oil fields: North Dakota Geological Survey, Miscellaneous Series 64.
- Sandberg, C.A., 1964, Precambrian to Mississippian paleotectonics of the southern Williston basin, (abs): Third International Williston Basin Symposium, Regina: Billings, Billings Geological Society, p. 37-38.
- Shinn, E.A., R.M. Lloyd, and R.N. Ginsburg, 1969, Anatomy of a modern carbonate tidal flat, Andros Island, Bahamas: Jour. Sed. Petrol., v. 39, p. 1202-1228.
- Smith, M.H., 1960, Revised nomenclature for the Williston basin: American Association of Petroleum Geologists Bulletin, v. 44, p. 959-960.
- Stone, D.S., and R.L. Hoeger, 1973, Importance of hydrodynamic factor in formation of Lower Cretaceous combination traps, Big Muddy-South Glenrock area, Wyoming: American Association of Petroleum Geologists Bulletin, v. 57, p. 1713-1733.
- Thode, H.G., 1981, Sulfur isotope ratios in petroleum research and exploration: Williston basin: American Association of Petroleum Geologists Bulletin, v. 65, p. 1527-1535.
- Thomas, G.E., 1974, Lineament tectonics; Williston-Blood Creek Basin: American Association of Petroleum Geologists Bulletin, v. 58, p. 1305-1322.
- Waples, D.W., 1980, Time and temperature in petroleum formation: application of Lopatin's method to exploration: American Association of Petroleum Geologists Bulletin, v. 64, p. 916-926.
- Webster, R.L., 1984, Petroleum source rocks and stratigraphy of the Bakken Formation in North Dakota, in Hydrocarbon Source Rocks of the Greater Rocky Mountain Region: Rocky Mountain Assoc. Geologists, Denver, Colorado, p. 57-81.

- Williams, J.A., 1974, Characterization of oil types in the Williston basin: American Association of Petroleum Geologists Bulletin, v. 58, p. 1243-1252.
- Willis, D.G., 1961, Entrapment of petroleum, in G. B. Moody, ed., Petroleum Exploration Handbook, New York, McGraw-Hill, chapter 6.
- Wilson, J.L., 1975, Carbonate Facies in Geologic History, New York, Springer-Verlag, 469 p.

APPENDICES

These appendices include the following:

Appendix A - Drill Stem Test Reports

Appendix B - Drill Stem Test Interpretations

APPENDIX A

Drill Stem Test Reports

The following abbreviations and symbols are used:

Elev: elevation of kelly bushing, (g)
denotes ground elevation.

Fluid Properties: water salinity in parts
per million; oil gravity in degrees
API.

BHT: bottom hole temperature in degees F.

APPENDIX A

DRILL STEM TEST REPORT

Well Operator/Number	Location spot/section	Elev. ft	Interval ft	Fluid Recovery ft (bbls)	Fluid Properties	BHT	Date
T140N R98W							
SunBehn 26-5	sw nw / 26	2533	9168-9202	180 inhibitor 180 mud	200,000+	220	06/82
Coastal BN-1	ne ne / 27	2548	9197-9235	233 water 7(bbls) emulsion 2(bbls) water	200,000+	237	07/81
T140N R99W							
Dover Cym.-1	----- / 03	2724	9600-9640	2(bbls) inhibitor 8(bbls) water	100,000	236	10/82
Farmers 2-13	nw ne / 13	2627	9470-9520	174 mud 272 water	-----	226	07/70
T140N R100W							
Conoco Fed. 2-1	sw nw / 02	2744g	9760-9817	755 mud c/water 465 water c/mud	-----	418	04/80
Chambers GC 1-8	ne nw / 08	2579	9400-9444	787 water	100,000	240	01/81
Rubco Fed. 22-12	----- / 22	2766	9556-9594	940 water cushion 360 mud c/oil 120 water	75,000	240	10/68

APPENDIX A (cont.)

Well Operator/Number	Location spot/section	Elev. ft	Interval ft	Fluid Recovery ft (bbls)	Fluid Properties	BHT	Date
T140N R102W							
Amerada Mel. 1	sw nw / 30	2583	9129-9164	75 oil 689 water cushion 720 water 180 mud	35 @ 60 25,000	222	03/69
Amerada Mel. 1	sw nw / 30	2583	9256-9425	1091 water cushion 7556 water	35,000	195	03/69
T140N R103W							
Indrex Ryd. 1	se sw / 13	2500	9065-9162	8473 oil, water	-----	220	06/81
Indrex Ryd. 1	se sw / 13	2500	9172-9204	270 muddy water 3092 water	22,000	222	06/81
Kewanee Fed. 1	se ne / 13	2445g	9136-9198	372 mud 5851 water	8,000	234	12/67
Shell St. 1	---- / 16	2618	9134-9183	15 oil 84 mud 1651 oil c/water	-----	215	08/69
Shell Gov. 14-20	---- / 20	2652	9150-9220	217 mud 1485 water	-----	218	10/67
Anadarko A-1	nw sw / 23	2458	9054-9100	95 mud 7616 water	80,000	217	03/82
Anadarko A-1	nw sw / 23	2458	9115-9145	948 mud c/water	80,000	219	03/82
Anadarko A-1	nw sw / 23	2458	9175-9272	200 water c/mud	8,000	222	03/82

APPENDIX A (cont.)

Well Operator/Number	Location spot/section	Elev. ft	Interval ft	Fluid Recovery ft (bbls)	Fluid Properties	BHT	Date
Hunt 1	nw sw / 24	2452	9026-9070	651 oil 1126 mud c/oil 186 water c/ oil 1953 water	23 @ 60	192	10/71
Hunt A 1	nw ne / 26	2443	8992-9018	210 mud c/ water 2475 water	7,000	234	05/72
Mesa Fed. 1-35	ne sw / 35	2484g	9014-9021	5425 water	35,000	220	06/81
Mesa Fed. 1-35	ne sw / 35	2484g	8960-8990	2142 water 930 mud c/ water	22,000	230	06/81
Kissinger 1-36	ne ne / 36	2519	9060-9080	180 mud c/ oil 570 mud c/ water 480 water	24.7 @60 200,000	180	01/78
T141N R98W							
Adobe 21-6	ne nw / 06	2597	9600-9650	120 oil, water 3331 water	200,000	238	02/82
Adobe 41-6	ne ne / 06	2587g	9585-9625	26(bbls) oil 18(bbls) water	39.4 @60 200,000	240	11/81
Gulf Kor. 1	---- / 08	2568g	9570-9607	35 oil 2708 gas c/water	150,000	220	04/78
Gulf 1-19-1A	nw nw / 19	2584	9550-9605	70 mud 5435 water	85,000	200	10/81
Nucorp 1	se ne / 32	2606g	9565-9601	246 mud 629 water	200,000	215	01/82

APPENDIX A (cont.)

Well Operator/Number	Location spot/section	Elev. ft	Interval ft	Fluid Recovery ft (bbls)	Fluid Properties	BHT	Date
T141N R99W							
Adobe 22-28	se nw / 28	2664g	9656-9708	279 mud 2052 water	200,000	250	11/81
Adobe 23-31	ne sw / 31	2734g	9610-9661	28(bbls) oil 8(bbls) water	45 @ 60 45,000	246	04/82
T141N R100W							
Hunt Arm #1	sw nw / 02	2741	9600-9641	150 mud 90 water	160,000	236	12/81
Al-Aquitaine 1-3	ne nw / 03	2526	9404-9437	--- mud,water	160,000	244	10/80
Al-Aquitaine 1-3	ne nw / 03	2526	9382-9410	3161 mud 30 water	-----	240	10/80
Al-Aquitaine 3-3	nw ne / 03	2589g	9460-9516	2035 mud emul. 300 water	160,000?	244	03/81
Shell 41-4	ne ne / 04	2510	9360-9438	35(bbls) oil 55(bbls) mud 1(bbl) water	43 @ 60	223	06/81
Al-Aquitaine 1-5	ne nw / 05	2453g	9393-9428	930 mud 6091 water	120,000	252	12/80
Al-Aquitaine 1-5	ne nw / 05	2453g	9348-9399	655 mud 2282 water	100,000	254	12/80
Al-Aquitaine 1-5	ne nw / 05	2453g	9314-9326	1707 mud oil c/ water	100,000	245	12/80
Getty MC 6-B	sw nw / 06	2470	9295-9361	85(bbls) oil 26(bbls) water etc	34 @ 60	246	09/79

APPENDIX A (cont.)

Well Operator/Number	Location spot/section	Elev. ft	Interval ft	Fluid Recovery ft (bbls)	Fluid Properties	BHT	Date
Getty MC B6-13	sw sw / 06	2500	9311-9370	99(bbls) oil 8(bbls) water etc	43 @ 60	250	05/80
Al-Aquitaine 1-7	nw nw / 07	2474	9326-9362	475 mud 849 water	175,000?	250	02/80
Al-Aquitaine 1-7	nw nw / 07	2474	9316-9344	90 oil 1013 water cushion 478 water	35 @ 60-	226	02/80
Al-Aquitaine 1-7	nw nw / 07	2474	9375-9410	1270 water	125,000	248	02/80
Shell 33-8	nw se / 08	2469	9362-9416	685 water cushion 50 water	-----	236	11/80
Shell 33-8	nw se / 08	2469	9254-9360	-----	-----	230	11/80
Adobe 14-11	sw sw / 11	2674	9520-9561	750 gas 178 gas c/ mud 93 gas c/ water	-----	244	03/82
Adobe 12-14	sw nw / 14	2751g	9560-9640	279 mud 660 mud c/ water	130,000?	240	10/81
Burlington 23-15	ne sw / 15	2536	9352-9390	933 water c/ oil	44 @ 60	236	06/81
Al-Aquitaine 1-16	ne se / 16	2494	9382-9301	9.6(bbls) oil 5.7(bbls) water 5.6(bbls) mud	40 @ 60 45,000	240	08/79
Al-Aquitaine 1-16	ne se / 16	2494	9328-9374	7.7(bbls) oil 3.5(bbls) water	43 @ 60 80,000	256	08/79
Al-Aquitaine 2-16	ne ne / 16	2535g	9273-9438	246 mud 400 mud c/ water 510 water	75,000	245	06/81
Al-Aquitaine 1-19	sw se / 19	2495	9290-9342	1455 mud 633 water	120,000	236	05/80

APPENDIX A (cont.)

Well Operator/Number	Location spot/section	Elev. ft	Interval ft	Fluid Recovery ft (bbls)	Fluid Properties	BHT	Date
Shell 1-2	se ne / 21	2668	9500-9566	265 mud	-----	150	06/59
Al-Aquitaine 1-22	ne ne / 22	2650	9460-9506	135 mud c/ water 15.7(bbls) oil	-----	240	07/79
Al-Aquitaine 2-22	ne sw / 22	2520	9388-9398	13(bbls) mud 1860 gas	50,000	244	08/79
Al-Aquitaine 2-22	ne sw / 22	2520	9332-9380	796 water 0.99(bbls) mud	43 @ 60	240	08/79
Al-Aquitaine 3-22	se nw / 22	2517	9328-9376	2.25(bbls) oil 0.38(bbls) water	43 @ 60	243	03/80
Al-Aquitaine 1-23	sw nw / 23	2545	9397-9422	3(bbls) mud 14.2(bbls) oil	43 @ 60	244	05/80
Al-Aquitaine 1-23	sw nw / 23	2545	9423-9439	3(bbls) water 619 mud	130,000	244	05/80
Supron F-26-2	nw sw / 26	2753g	9430-9513	90 water 563 mud	-----	250	05/80
Al-Aquitaine 1-27	se sw / 27	2638	9440-9475	520 mud c/ water	75,000	244	03/81
Al-Aquitaine 2-27	sw ne / 27	2681	9464-9507	620 water 1107 mud	-----	248	03/80
Al-Aquitaine 2-27	sw ne / 27	2681	9513-9621	1107 mud 3093 gas c/oil	44 @ 60	250	05/81
Al-Aquitaine 3-27	se nw / 27	2683g	9435-9477	1107 mud 1172 oil	42 @ 60	247	05/81
				1014 water 1084 mud	70,000		
				718 emulsion	-----	244	07/81

APPENDIX A (cont.)

Well Operator/Number	Location spot/section	Elev. ft	Interval ft	Fluid Recovery ft (bbls)	Fluid Properties	BHT	Date
Al-Aquitaine 1-28	ne ne / 28	2685	9512-9528	300 mud 360 water	-----	240	05/80
Al-Aquitaine 1-28	ne ne / 28	2685	9499-9513	8589 gas 860 gas c/ oil	43 @ 60	240	05/80
Al-Aquitaine 1-30	ne nw / 30	2470	9260-9301	6.9(bbls) oil 3.3(bbls) water	38 @ 60 110,000	239	09/79
Al-Aquitaine 1-30	ne nw / 30	2470	9312-9324	737 mud c/ water	-----	236	09/79
J Chambers 2-31	sw ne / 31	2479g	9232-9288	2.9(bbls) oil 1.6(bbls) water	-----	230	10/79
J Chambers 2-31	sw ne / 31	2479g	9296-9338	180 mud 2935 water	140,000	248	10/79
Al-Aquitaine 11-33	ne sw / 33	2493g	9230-9286	433 mud	-----	238	09/81
Al-Aquitaine 11-33	ne sw / 33	2493g	9285-9335	910 water	100,000	238	09/81
Al-Aquitaine 1-33	ne ne / 33	2529	9298-9348	35 oil 707 mud c/ oil	42 @ 60	240	12/80
Conoco 33-2	ne nw / 33	2523	9300-9390	2253 water	50,000	250	09/80
Mesa FED 1-34	----- / 34	2592	9366-9426	360 mud	-----	243	12/69
T141N R101W							
Getty MC 1-3	nw nw / 1	2480g	9272-9298	246 mud 934 water	14,000	240	06/80
Getty MC 1-3	nw nw / 01	2480	9216-9252	4.5(bbls) water	175,000	251	06/80
Getty MC 1-1	ne ne / 01	2456	9256-9312	93(bbls) oil	35 @ 60	222	03/79
Getty MC 1-11	ne sw / 01	2518	9292-9352	? gas c/oil ? mud emulsion	-----	230	09/79

APPENDIX A (cont.)

Well Operator/Number	Location spot/section	Elev. ft	Interval ft	Fluid Recovery ft (bbls)	Fluid Properties	BHT	Date
Getty FED 1-16	---- / 01	----	9283-9343	71(bbls) oil	35 @ 60	238	01/80
Tenneco Oyhus 1-2	sw nw / 02	2347g	9121-9182	998 oil	39 @ 60	230	04/81
				249 water	80,000		
Coastal BN 1	ne se / 03	2400g	9190-9256	761 gas c/oil	100,000	238	03/82
				2612 gas c/ water			
Al-Aquitaine 3-11	se ne / 11	2520	9295-9355	560 gas c/ water	140,000	230	02/81
				2740 gas c/ oil	36 @ 60		
Al-Aquitaine 4-11	ne nw / 11	2500	9298-9350	95 oil	90,000	240	02/81
				915 mud			
				1030 water			
Al-Aquitaine 1-11	ne sw / 11	2505	9296-9348	11(bbls) water	80,000	239	03/79
				4.7(bbls) emulsion			
J Chambers 4-12	nw nw / 12	2496	9338-9386	581 mud	110,000	218	12/79
				280 water			
J Chambers 4-12	nw nw / 12	2496	9280-9332	1068 oil	41 @ 60	220	12/79
				267 mud			
Al-Aquitaine ST-1	se nw / 13	2595	9127-9257	498 mud	36 @ 60	236	07/78
				1122 emulsion			
				651 gas c/ oil			
				353 water			
Al-Aquitaine ST-1	se nw / 13	2595	9387-9440	-----	-----	238	07/78
Chambers 2-14X	se se / 14	2501	9279-9306	1302 mud	120,000	226	03/80
				775 emulsion			
				465 oil			
				93 water			

APPENDIX A (cont.)

Well Operator/Number	Location spot/section	Elev. ft	Interval ft	Fluid Recovery ft (bbls)	Fluid Properties	BFT	Date
Al-Aquitaine 1-14	ne ne / 14	2660	9455-9508	1842 oil 431 water 420 mud	40 @ 60 105,000	236	02/79
Al-Aquitaine 1-14	ne ne / 14	2660	9515-9530	809 water	45,000	236	02/79
Al-Aquitaine 2-14	ne nw / 14	2592	9371-9420	676 mud 904 gas c/ oil 3044 water	40 @ 60 100,000	240	03/80
Chambers FCS 1-14	ne sw / 14	2503	9390-9415	309 mud c/ water 2823 water	48,000	253	08/78
Chambers ST-2-14X	se se / 14	2501	9318-9338	1240 gas c/ oil	37 @ 60	234	03/80
Chambers ST-2-14X	se se / 14	2501	9368-9381	939 mud 1548 mud c/ oil 601 water	70,000	240	03/80
Chambers ST-2-14X	se se / 14	2501	9402-9422	1473 mud c/ water 2433 water	25,000	249	03/80
Chambers ST-1-15	se se / 15	2436	9219-9274	799 gas c/ oil 701 oil c/ water	36 @ 60 52,000	236	10/78
Chambers ST-1-15	se se / 15	2436	9280-9294	1133 oil 600 oil c/ water 320 water	39 @ 60 40,000	242	10/78
Chambers NDST-1-22	sw ne / 22	2399	9264-9288	3593 water	10,000	242	08/78
Chambers FCS-1-23	ne nw / 23	2504	9225-9340	7000 oil	39 @ 60	243	07/78
Chambers FCS-1-23	ne nw / 23	2504	9378-9470	510 mud 279 mud c/ water 7216 water	24,000?	266	07/78
Chambers NDST-2-23	se ne / 23	2499	9380-9404	373 mud 620 gas c/ water	60,000	234	04/79

APPENDIX A (cont.)

Well Operator/Number	Location spot/section	Elev. ft	Interval ft	Fluid Recovery ft (bbls)	Fluid Properties	BHT	Date
Chambers ST-4-23	se sw / 23	2346	9169-9209	6804 emulsion	-----	260	10/78
Al-Aquitaine 3-24	nw sw / 24	2482	9285-9339	3070 gas	-----	230	12/78
Al-Aquitaine 1-24	se ne / 24	2514	9047-9177	558 mud 564 water	-----	228	09/78
Al-Aquitaine 1-24	se ne / 24	2514	9313-9364	539 oil, mud	-----	238	09/78
Al-Aquitaine 1-24	se ne / 24	2514	9377-9396	184 mud 276 water	50,000	239	09/78
Al-Aquitaine 4-24	nw nw / 24	2498	9308-9364	17.3(bbls) oil 0.6(bbls) water 1.0(bbls) mud	36 @ 60	237	01/80
Patrick M-1-25	sw nw / 25	2384	8947-8992	186 mud 452 mud c/ water	90,000	222	11/80
Patrick M-1-25	sw nw / 25	2384	9156-9202	969 emulsion	-----	240	11/80
Patrick H-4-27	nw sw / 27	2516	9294-9360	372 mud 1617 water	45,000	238	09/81
Patrick H-1-27	nw se / 27	2507g	9014-9071	906 mud, oil 180 mud, water	-----	234	04/81
Patrick H-1-27	nw se / 27	2507g	9220-9282	558 mud etc. 621 water	80,000	235	05/81
Patrick H-1-27	nw se / 27	2507g	9280-9320	2000 emulsion 2564 oil 912 water	34 @ 60 27,500	248	05/81
Patrick H-2-27	sw nw / 27	2412	9197-9214	2218 oil 950 water	34 @ 60 14,000	248	08/81
Patrick H-3-27	se ne / 27	2456	9214-9276	2050 oil, water 1494 oil 415 water	40 @ 60	238	06/81

APPENDIX A (cont.)

Well Operator/Number	Location spot/section	Elev. ft	Interval ft	Fluid Recovery ft (bbls)	Fluid Properties	BHT	Date
Patrick H-4-27	nw sw / 27	2516	9294-9360	372 mud 1617 water	25,000	238	09/81
T141N R102W							
Al-Aquitaine 1-9	ne sw / 09	2467	9155-9230	460 mud 3620 water cut mud	80,000	212	03/80
Al-Aquitaine 1-9	ne sw / 09	2467	9231-9275	10 mud 2304 water	80,000	220	04/80
Al-Aquitaine 1-10	sw sw / 10	2408g	9179-9199	2268 mud 280 water cut mud 373 water	70,000	218	10/81
Cenex FED-12-29	nw sw / 29	2607g	9210-9232	4180 water	-----	205	09/79
Cenex FED-12-29	nw sw / 29	2607g	9260-9285	240 mud cut water 1244 water	53,000	210	09/79
Patrick H-F 1-30	ne se / 30	2603	9196-9241	180 gas cut oil 314 oil cut mud 1767 water	15,500	205	03/81
T142N R98W							
Anadarko REP-A-1	sw se / 03	2758g	9848-9883	80 mud 150 water	160,000	233	07/82
Adobe STK-34-31	sw se / 31	2615	9585-9645	120(bbls) oil 15(bbls) water	42 @ 60	231	06/81
Gulf SSL-2-36	nw sw / 36	2674	9638-9669	182 mud	-----	224	05/77
Gulf SSL-2-36	nw sw / 36	2674	9867-9965	2683 water	200,000	240	05/77

APPENDIX A (cont.)

Well Operator/Number	Location spot/section	Elev. ft	Interval ft	Fluid Recovery ft (bbls)	Fluid Properties	BHT	Date
T142N R99W							
Hunt Baranko-1	nw ne / 03	2728	9857-9948	3433 water	200,000+	250	04/80
T142N R100W							
Koch FED-6-3	se nw / 03	2793g	9716-9752	15(bbls) oil	42 @ 60	245	04/80
Koch FED-7-3	sw ne / 03	2778g	9705-9734	flowed oil, water	42 @ 60	235	04/81
Pentad R-1	se ne / 04	2721g	9612-9663	93 mud	180,000	252	10/80
				2486 water			
Hunt R-A-1	se se / 04	2813g	9741-9806	-----	-----	222	04/80
Hunt R-A-1	se se / 04	2813g	9750-9762	190 mud	-----	260	04/80
Koch Kordon-4-5	sw sw / 05	2722	9628-9654	450 water	-----	312	06/79
				1580 mud cut oil			
Koch FED-6-6M	se nw / 06	2751	9634-9673	mud, water + oil	-----	252	11/79
Koch FED-6-6M	se nw / 06	2751	9707-9724	70 mud	200,000+	240	11/79
				100 water			
Koch FED-10-6	nw se / 06	2690	9664-9682	30(bbls) oil	41 @ 60	250	11/79
Koch FED-K-15-6	sw se / 06	2747	9624-9661	79(bbls) oil	36 @ 60	256	12/79
Brown FED-8-12X	nw nw / 08	2639	9500-9620	837 mud	60,000?	---	08/80
				5963 water			
Supron SND-1	sw ne / 09	2757	9640-9710	300 mud	170,000	252	04/80
				536 emulsion			
				7522 water			
Supron SND-1	sw ne / 09	2757	9637-9669	180 water	85,000	---	04/80
Hunt Gregory-1	sw ne / 10	2782	9650-9742	oil + mud	44 @ 60	246	07/79
Hunt Osadchuch-2	se se / 15	2733g	9636-9692	77(bbls) oil	43 @ 60	240	10/79

APPENDIX A (cont.)

Well Operator/Number	Location spot/section	Elev. ft	Interval ft	Fluid Recovery ft (bbls)	Fluid Properties	BHT	Date
Hunt Fritz-1	ne ne / 22	2750	9570-9660	42(bbls) oil 10(bbls) water	42 @ 60	250	04/79
Hunt Fritz-1	ne ne / 22	2750	9672-9770	3630 water	-----	250	05/79
Hunt Osadchuck-1	sw nw / 23	2740	9584-9660	75(bbls) oil	40 @ 60	256	09/79
Hunt Osadehuk	-----/ 23	2704	9616-9647	287 mud 272 water	140,000	238	05/80
Hunt Anheluk-ST-2	sw se / 23	2688g	9655-9683	186 mud 380 gas cut mud	200,000	234	06/80
Patrick 1-26	sw nw / 26	2756	9640-9692	3000 gas 540 mud 93 water	90,000	238	04/80
Koch FED-1-27	ne ne / 27	2713	9603-9638	-----	-----	305	01/80
Patrick FED-2-28	sw ne / 28	2631g	9510-9570	3199 oil 375 mud cut oil	-----	242	02/81
Supron NDST-2	ne sw / 28	2717g	9592-9633	46.5(bbls) emul. 3.9(bbls) water	44 @ 60	248	03/81
Koch FED-10-31	nw se / 31	2450	9304-9339	43(bbls) oil 7(bbls) water	39 @ 60	250	04/80
Patrick FED-2-32	sw nw / 32	2486	9404-9429	123 mud 1047 water	90,000	245	09/80
Patrick FED-2-32	sw nw / 32	2486	9310-9328	1472 mud	-----	232	08/80
Patrick FED-1-32	ne sw / 32	2462	9280-9348	60(bbls) oil 1.3(bbls) water	43 @ 60	261	06/80
Koch FED-1-33	sw ne / 33	2513	9360-93998	-----	-----	200	02/80
Supron Cerkoney-3	nw se / 34	2648	9494-9553	30(bbls) oil	44 @ 60	232	02/80
Supron Cerkoney-1	nw sw / 34	2580	9410-9442	23.5(bbls) oil 6(bbls) emulsion	36 @ 60	---	11/79

APPENDIX A (cont.)

Well Operator/Number	Location spot/section	Elev. ft	Interval ft	Fluid Recovery ft (bbls)	Fluid Properties	BHT	Date
Supron Cerkoney-4	nw ne / 34	2659	9540-9586	1126 emulsion 180 mud cut water	40 @ 60	241	05/80
Supron FED-1-35	ne sw / 35	2737	9680-9772	795 mud cut water 282 emulsion 94 oil cut mud	200,000	242	09/79
Supron FED-2-35	nw sw / 35	2748	9622-9666	-----		220	11/80
Supron FED-3-35	nw nw / 35	2774	9630-9688	1645 oil + water 579 mud + water 432 mud	200,000	246	06/81
T142N R101W							
Anderson FED-1-1	ne se / 01	2663	9550-9595	186 gas cut mud 4086 water	75,000	240	01/81
Conoco FED-H-8-1	ne se / 08	2430	9284-9334	372 mud 372 mud cut water 455 water	120,000	190	02/81
Brent FED-11	ne sw / 12	2445	9353-9370	911 water 180 mud 563 sulfur water 10 oil		265	08/79
Koch FED-16-14	se se / 14	2522	9374-9408	704 oil 180 mud 1062 water	75,000	250	07/81
Coastal BN-1	se se / 15	2501	9304-9377	500 mud cut water 1500 oil emul. 2000 water	90,000	245	11/81

APPENDIX A (cont.)

Well Operator/Number	Location spot/section	Elev. ft	Interval ft	Fluid Recovery ft (bbls)	Fluid Properties	BHT	Date
Milestone BN-23-23	ne sw / 23	2544	9390-9406	1916 water	200,000?	232	08/81
Milestone BN-23-23	ne sw / 23	2544	9382-9420	3619 water	60,000	250	08/81
Milestone BN-23-23	ne sw / 23	2544	9390-9406	1422 gas cut water	58,000	212	08/81
Coastal BN-3	se nw / 23	2682	9500-9569	75(bbls) oil	34 @ 60	245	03/81
Koch FED-8-24	se ne / 24	2522	9337-9367	93(bbls) oil	42 @ 60	264	11/79
Koch FED-9-24	ne se / 24	2458	9350-9380	85(bbls) oil	37 @ 60	260	09/79
Koch FED-13-24	sw sw / 24	2543g	9375-9401	flow oil + gas	38 @ 60	250	02/80
Getty MC-A-36-2	nw ne / 36	2530	9320-9386	70(bbls) oil 10(bbls) water	36 @ 60	238	11/79
Getty MC-A-36-10	nw se / 36	2505	9300-9356	25(bbls) oil 2(bbls) water	39 @ 60	230	06/79
T142N R102W							
Shamrock FED-34-4	sw se / 04	2556	9170-9229	243 cushion 1020 water	80,000	224	03/81
Shamrock FED-34-4	sw se / 04	2556	9390-9504	243 cushion 651 gas cut mud 1485 water	140,000	236	03/81
Shamrock RS-21-9	ne nw / 09	2536	9395-9427	62 mud cut water 827 water	100,000?	215	07/80
Mackoff 23-17	ne sw / 17	2606	9441-9468	429 mud 372 gas cut water 372 water cut mud 154 water		212	03/80
Mackoff 23-17	ne sw / 17	2606	9373-9393	652 mud 515 water	-----	190	03/80

APPENDIX A (cont.)

Well Operator/Number	Location spot/section	Elev. ft	Interval ft	Fluid Recovery ft (bbls)	Fluid Properties	BHT	Date
Cenex FED-14-26	se sw / 26	2264	9080-9122	2816 water	200,000	226	08/79
T143N R98W							
Amoco 1-1	ne ne / 04	2475	9630-9734	8000 oil cut water	100,000	220	02/80
Amoco 1-1	/ 28	2682g	9817-9895	1800 cushion 2314 water	165,000	235	09/78
Amarex Krogh-1	sw nw / 34	2692	9820-9870	350 gas 246 gas cut water 1112 water	200,000+	227	05/82
Mosbacher GS-1-36	ne nw / 36	2690	9826-9890	500 cushion 270 mud 389 water	200,000	228	09/78
Mosbacher GS-1-36	ne nw / 36	2690	9766-9830	30 oil 527 oil + cushion 595 mud cut water	41 @ 60	226	09/78
T143N R99W							
Amoco Hecker-1	-----/ 02	2717	9920-9970	9800 mud		282	02/80
Amoco 1-1	se se / 09	2742	9880-9964	1550 water 910 mud cut water	200,000	210	11/78
Amoco Knudtson-1	ne ne / 21	2730	9916-9971	740 cushion 5119 water	91,000	244	04/80
Hunt Demanion-1	se sw / 34	2747	9870-10010	3504 gas cut water	200,000	242	12/80

APPENDIX A (cont.)

Well Operator/Number	Location spot/section	Elev. ft	Interval ft	Fluid Recovery ft (bbls)	Fluid Properties	BHT	Date
T143N R100W							
Al-Aquitaine BN5-1	se nw / 05	2418	9315-9356	186 oil cut mud 26 oil cut water	200,000+	248	05/78
Al-Aquitaine 1-8	nw ne / 08	2461	9410-9450	373 mud cut water	200,000	236	07/80
Al-Aquitaine 1-8	nw ne / 08	2461	9454-9490	93 mud cut water 2124 water	200,000	258	07/80
Davis J-FED-1	se se / 08	2696g	9669-9686	295 gas cut oil 190 mud + oil 592 water	40 @ 60 200,000	238	05/82
Al-Aquitaine 1-16	se se / 16	2719g	9719-9747	6783 water	125,000	262	08/81
Gulf DC-1-18-1A	nw nw / 18	2749	9712-9725	558 cushion 150 water cut mud	-----	235	03/80
Gulf DC-1-18-1A	nw nw / 18	2749	9742-9822	199 cushion 5982 water	200,000	250	03/80
Everett FED-5-22	sw nw / 22	2736	9615-9668	450 gas cut water 1250 water	90,000	260	09/81
Coastal Y-23-1	nw nw / 23	2599g	9582-9636	180 mud 940 water	140,000	260	04/81
Hunt Johnson-1	nw se / 27	2701	9658-9710	2311 water + mud	150,000	256	07/81
Tenneco BN-1-29	ne sw / 29	2642	9542-9578	4255 gas cut oil 704 water	42 @ 60 200,000	260	10/77
Tenneco G-1-30	se ne / 30	2612	9489-9571	464 mud 279 mud cut water 3650 water		243	12/77

APPENDIX A (cont.)

Well Operator/Number	Location spot/section	Elev. ft	Interval ft	Fluid Recovery ft (bbls)	Fluid Properties	BHT	Date
Tenneco FED-2-30	se se / 30	2677	9565-9582	1486 cushion 130 oil 1172 water	145,000 35 @ 60	256	06/78
Apache BN-2-31B	sw se / 31	2756	9673-9690	1732 water	-----	297	03/80
Apache BN-2-31B	sw se / 31	2752	9654-9672	90 mud 535 water	175,000	238	03/80
Koch Simmioniw-2	nw se / 32	2716	9597-9623	flow oil + gas	42 @ 60	248	03/79
Koch Simmioniw-1	sw ne / 32	2702	9577-9607	6000 gas cut oil	30 @ 60	246	02/79
Hunt Kordon-2	nw sw / 32	2736	9598-9671	32 (bbls) oil 29 (bbls) water	34 @ 60	260	04/79
Farmers FED-4-33	nw nw / 33	2680	9555-9617	1780 water	100,000	235	03/78
Koch FED-5-33	sw nw / 33	2790	9608-9632	90 mud 180 muddy water 2815 water	-----	235	08/79
Patrick H-1-34	sw sw / 34	2723	9435-9471	175 mud 600 mud cut water	175,000	---	07/81
Koch FED-15-34	sw se / 34	2742	9642-9667	280 oil emulsion 870 gas cut oil	41 @ 60	240	06/81
Hunt Fedora-1	nw ne / 34	2746g	9664-9695	2939 gas cut oil	43 @ 60	230	09/81
T143N R101W							
Samson FED-1-2	sw sw / 02	2373	9438-9464	249 mud 1662 water	160,000	250	10/79
Farmers FED-11-4	ne sw / 04	2429	9390-9407	1198 cushion 290 water	180,000	239	11/78

APPENDIX A (cont.)

Well Operator/Number	Location spot/section	Elev. ft	Interval ft	Fluid Recovery ft (bbls)	Fluid Properties	BHT	Date
Farmers FED-11-4	ne sw / 04	2429	9332-9356	1195 cushion 96 mud 90 water	190,000	236	11/78
Apache FED-13-4	sw sw / 04	2353	9303-9342	125 gas cut oil 2050 water	125,000	250	06/79
Cenex FED-2-4	nw ne / 04	2455g	9409-9421	68 (bbls) oil	44 @ 60	248	11/81
Apache 1-8	ne se / 08	2455	9310-9370	62 mud 992 water	180,000	195	03/79
Cenex FED-14-8	se sw / 08	2404	9295-9371	692 mud + water	200,000	228	02/80
Cenex FED-14-8	se sw / 08	2404	9376-9450	916 water	190,000	240	02/80
Apache 1-9	ne sw / 09	2445	9382-9404	3175 gas cut oil 348 oil emulsion 916 mud cut water	40 @ 60	230	07/79
Cenex Fed-12-10	nw sw / 10	2476	9432-9445	207 gas cut oil 385 gas + oil 153 water	200,000 40 @ 60	228	01/81
Apache ST-1-16	ne sw / 16	2493	9459-9472	423 oil cut mud 282 gas cut mud 911 water		170?	11/79
Apache ST-4-16	nw se / 16	2501	9477-9488	93 mud 624 water	200,000+	230	06/80
Apache ST-3-16	nw ne / 16	2526	9490-9519	865 oil + water	23 @ 60	226	06/80
Apache Fed-4-17	sw sw / 17	2444	9399-9420	371 mud 1351 water	200,000+	240	05/80
Apache FED-4-17	sw sw / 17	2444	9322-9404	180 gas cut oil 1400 cushion 581 gas cut water	200,000 37 @ 60	238	04/80

APPENDIX A (cont.)

Well Operator/Number	Location spot/section	Elev. ft	Interval ft	Fluid Recovery ft (bbls)	Fluid Properties	BHT	Date
Chambers BFED-3-19	sw sw / 19	2373	9300-9369	351 mud 3317 water	200,000	240	06/80
Tenneco BN-1-25	nw nw / 25	2555	9528-9557	800 cushion 3850 water	155,000	258	07/77
Chambers BU-2-27	sw sw / 27	2480g	9365-9420	1200 mud		240	09/81
Chambers BFED-1-28	se nw / 28	2405g	9400-9440	180 mud 1627 water	150,000	240	08/79
T143N R102W							
Cenex BN-5-1	sw nw / 01	2300	9263-9273	180 oil cut water 1250 water	190,000	242	01/80
Cenex BN-5-1	sw nw / 01	2300	9228-9242	660 water		230	01/80
Cenex Connell-6-2	se nw / 02	2277	9188-9255	180 gas cut mud 180 mud cut water 1206 water	150,000	234	08/80
Cenex Connell-6-2	se nw / 02	2277	9253-9280	90 mud 1101 water	150,000	235	08/80
Apache FED-1-5	ne se / 05	2155	9145-9158	60 mud cut water 1554 water	200,000	212	06/79
Conoco FEDB-13-1	se se / 13	2344g	9268-9318	180 cushion 2187 mud		223	04/81
N.A.Royalties R-1	----- / 22	----	9310-9333	270 muddy water 1110 water			02/58
Al-Aquitaine BN-1	----- / 23	2300g	9220-9337	360 mud cut water 1731 water	110,000	233	07/81

APPENDIX A (cont.)

Well Operator/Number	Location spot/section	Elev. ft	Interval ft	Fluid Recovery ft (bbls)	Fluid Properties	BHT	Date
T143N R103W							
Grace FED-52-22	sw ne / 22	2455g	9295-9331	180 cushion 700 water	140,000	268	11/81
Fayette BC-24-23	----- / 24	2530	9379-9410	180 mud 1105 water	85,000	221	12/81
Shamrock W-F-24-25	se sw / 25	2595	9369-9385	300 oil cut mud 393 water	-----	224	02/79
Shamrock W-F-24-25	se sw / 25	2595	9395-9415	1300 cushion 180 mud 644 water	-----	---	03/79
Shamrock W-F-24-25	se sw / 25	2595	9421-9451	1252 water	110,000	224	02/79
Gas Prod. ST-1-1	nw nw / 36	2524	9334-9360	401 mud cut water 210 water	150,000	210	06/79
Gas Prod. ST-2	ne se / 36	2470	9267-9283	186 gas cut water		218	05/80
T144N R98W							
Gulf Miller #1-10	nw se / 10	2568g	9730-9801	2450 gas cut oil	39.7 @ 60	238	04/77
T144N R99W							
Amoco Tachenko #1	se se / 14	2731g	9942-10044	1929 cushion 2209 water	200,000+	247	08/77

APPENDIX A (cont.)

Well Operator/Number	Location spot/section	Elev. ft	Interval ft	Fluid Recovery ft (bbls)	Fluid Properties	BHP	Date
Supron H-D 1	sw ne / 21	2716	9898-9934	459 gas cut oil 1160 water	200,000+	257	07/81
Amoco Bl	nw se / 29	2676	9844-9915	2250 mud cut water	129,000	246	02/81
T144N R100W							
Patrick 1-4	sw ne / 04	2462g	9726-9751	93 mud cut water 1209 water		250	01/82
Patrick 1-4	sw ne / 04	2462g	9818-9864	465 mud 1580 water	190,000	250	01/82
Amoco Fed.1	se nw / 20	2558	9540-9608	1581 cushion 1674 water	200,000	220	09/79
Koch Fed. 13-30	sw sw / 30	2615	9646-9664	1074 water	200,000	237	01/80
Koch Fed. 13-30	sw sw / 30	2615	9599-9633	651 mud 186 gas cut water 909 mud cut water	200,000+	226	01/80
Koch Fed. 13-30	sw sw / 30	2615	9499-9580	1508 cushion 90 mud		280	01/80
Apache Fed. 33-31	nw se / 31	2403	9390-9430	130 mud 630 mud cut water	200,000	230	02/78
Apache Fed. 33-31	nw se / 31	2403	9540-9614	520 gas cut mud 90 mud		226	02/78
Jordan 1-1	se se / 36	2597	9730-9763	2000 cushion 1200 water		253	03/66
Jordan 1-1	se se / 36	2597	9770-9805	2000 water cushion 1574 water	200,000+	250	03/66

APPENDIX A (cont.)

Well Operator/Number	Location spot/section	Elev. ft	Interval ft	Fluid Recovery ft (bbls)	Fluid Properties	BHT	Date
T144N R101W							
Supron 6-3	nw se / 06	2203	9228-9252	185 oil 715 water	200,000 35 @ 60	220	01/82
Supron 6-2	se ne / 06	2211	9220-9250	4 (bbls) oil 17 (bbls) water	163,000	284	12/80
Supron 7-1	nw ne / 07	2250	9250-9286	4126 oil + emul.	36 @ 60	240	06/81
Supron 7-1	nw ne / 07	2250	9318-9346	558 mud 6004 water	200,000+	240	06/81
Florida 8-2	ne nw / 08	2261	9310-9334	50 mud 750 gas cut water	200,000	232	06/82
Florida 8-3	ne nw / 08	2261	9270-9304	180 mud cut water 320 water	200,000	234	05/82
Koch 6-11	se nw / 11	2325	9356-9386	155 mud 279 mud cut water 302 water	200,000	240	05/80
Koch 6-11	se nw / 11	2325	9412-9441	90 mud cut water 2130 water	145,000	210	05/80
Northrop Al-13	sw sw / 13	2331	9456-9639	oil + water		230	02/80
Northrop Al-13	sw sw / 13	2331	9408-9445	240 chemicals 146 water cut mud		220	02/80
Amoco F-2	se sw / 15	2338g	9384-9374	5139 mud + chem.		217	10/80
Amoco F-2	se sw / 15	2338g	9384-9435	218 chemicals 180 muddy water 1289 water		---	10/80
Duncan 15-43	ne se / 15	2355	9409-9426	930 water	140,000		08/82

APPENDIX A (cont.)

Well Operator/Number	Location spot/section	Elev. ft	Interval ft	Fluid Recovery ft (bbls)	Fluid Properties	BHT	Date
Duncan 15-43	ne se / 15	2355	9351-9391	960 oil emulsion 200 water	200,000		08/82
Supron 18-1	sw ne / 18	2273g	9513-9540	2400 mud cut water		---	03/82
Supron 19-1	se sw / 19	2248	9208-9236	700 water cut mud		230	08/82
Florida 19-1	se sw / 19	2248	9244-9272	812 mud emulsion 2000 water	200,000	231	08/82
Koch 6-22	se nw / 22	2363	9336-9386	64 (bbls) oil 2 (bbls) cut oil	41 @ 60	240	05/81
Koch 6-22	se nw / 22	2363	9396-9410	182 mud cut water 469 water	200,000	243	05/81
Koch 13-22	sw sw / 22	2585	9592-9672	90 oil 900 mud cut oil	200,000 38 @ 60	220	11/80
Tenneco 2-28	se sw / 28	2270g	9244-9256	774 mud cut water 90 mud cut oil 232 gas cut oil 700 cushion 95 water	40 @ 60	226	09/81
Ladd 34-11	nw nw / 34	2318	9274-9356	1029 mud cut oil 1766 oil emulsion 650 gas cut oil 1407 water	175,000 34 @ 60	230	07/82
T144N R102W							
MGP 44-1	se se / 01	2308g	9325-9345	1000 cushion 601 gas cut oil 180 water	200,000 40 @ 60	232	07/81

APPENDIX A (cont.)

Well Operator/Number	Location spot/section	Elev. ft	Interval ft	Fluid Recovery ft (bbls)	Fluid Properties	BHT	Date
MGF 44-1	se se / 01	2308g	9385-9398	976 cushion 2813 water	180,000	248	07/81
MGF 42-1	se ne / 01	2233g	9252-9274	593 gas cut oil 85 water	40 @ 60	220	10/81
Apache 2-4	sw sw / 02	2524	9543-9580	350 gas cut mud 1399 gas cut water	200,000	---	08/81
Apache 2-4	sw sw / 02	2524	9604-9648	180 mud 1003 water		230	08/81
Texakota 1-2	----- / 02	2254	9276-9312	93 oil 1280 cushion 540 water	190,000 36 @ 60	242	08/73
Texakota 1-2	----- / 02	2254	9284-9327	60 oil cut water 1372 water	200,000	243	08/73
Apache 2-5	sw ne / 02	2395g	9440-9486	558 gas cut mud 640 gas cut water	120,000	---	03/82
Apache 3-2A	sw sw / 03	2234g	9253-9283	211 mud 840 water	200,000	236	11/81
Apache 3-2A	sw sw / 03	2234	9307-9354	195 mud 558 gas cut water	200,000	230	11/81
Apache 3-1	ne ne / 03	2521	9402-9447	1403 mud emulsion 180 water	200,000	248	10/80
Apache 3-1	ne ne / 03	2521	9473-9506	189 mud 698 mud emulsion 130 water emulsion 525 water	200,000	247	10/80

APPENDIX A (cont.)

Well Operator/Number	Location spot/section	Elev. ft	Interval ft	Fluid Recovery ft (bbls)	Fluid Properties	BHT	Date
Supron F-1	ne se / 10	2207g	9536-9580	630 gas cut mud 520 gas cut water 524 water	200,000	230	08/81
Supron F-1	ne se / 10	2207g	9610-9632	198 gas cut mud 1032 water	200,000	240	08/81
Florida 13-1	ne ne / 13	2689	9654-9685	234 oil 352 water	175,000 37 @ 60	230	07/82
Apache 2-14	sw sw / 14	2237	9208-9223	196 oil 1908 water	165,000 36 @ 60	205	11/80
Apache 2-14	sw sw / 14	2237	9234-9242	1436 mud emulsion 558 gas cut water 180 water	200,000	234	11/80
Apache 15-1	ne se / 15	2267	9216-9247	703 mud 2089 oil emulsion	39 @ 60	234	03/81
Apache 15-2	ne ne / 15	2521g	9519-9539	633 mud 563 oil 1195 oil emulsion 1983 water	38 @ 60	240	09/81
Tenneco 1-15	se sw / 15	----	9136-9183	540 cushion 867 emulsion 447 water	200,000	231	06/81
Apache 22-1	ne se / 22	2296	9293-9320	1911 mud 1561 water	180,000	239	02/81
Apache 22-1	ne se / 22	2296	9254-9284	1674 oil cut mud		226	02/81
Apache 1-22	ne ne / 22	2173	9151-9201	204 mud 563 gas cut oil 439 water	140,000 36 @ 60	236	05/80

APPENDIX A (cont.)

Well Operator/Number	Location spot/section	Elev. ft	Interval ft	Fluid Recovery ft (bbls)	Fluid Properties	BHT	Date
Apache 1-22	ne ne / 22	2173	9224-9280	103 mud 585 water	200,000	228	05/80
Apache 2-23	sw nw / 23	2176	9121-9133	467 mud		220	10/80
Apache 2-23	sw nw / 23	2176	9199-9215	701 mud 1527 water	175,000	230	10/80
Apache 2-23	sw nw / 23	2176	9136-9156	704 mud 733 water emulsion 90 water	140,000	230	10/80
Apache 23-3	ne sw / 23	2175	9148-9162	214 water cut mud 150 oil 555 water	110,000 35 @ 60	228	08/81
Apache 23-3	ne sw / 23	2175	9181-9189	1202 water	200,000	218	08/81
Apache 23-3	ne sw / 23	2175	9177-9189	1204 water	200,000	218	08/81
Apache 27-1	sw ne / 27	2198g	9200-9350	180 mud 280 water cut mud 1000 water	200,000	210	07/81
Apache 27-1	sw ne / 27	2198g	9195-9205	1377 mud		220	07/81
Apache 27-1	sw ne / 27	2198g	9172-9190	759 mud 496 water	200,000	155?	07/81
Coastal 1-29	nw nw / 29	2239	9194-9250	599 cushion 425 mud cut oil 500 chem. cut oil		110?	10/81

APPENDIX B

Drill Stem Test Interpretations

The following abbreviations and symbols are used:

Pressure measured: pressure from extrapolation of shutin pressure buildup.

Pressure corrected: pressures in oil column corrected to water column pressures

Head fresh: calculated freshwater hydrostatic head in ft; (*) denotes values used in regional potentiometric map Fig. 22.

Head corr.: calculated hydrostatic heads using corrected density values Fig. 26; (a) denotes corrected values used in Fig. 32.

APPENDIX B

FLUID PRESSURES FROM DRILL STEM TEST INTERPRETATION

Well Operator/Number	Location spot/section	Gauge		Pressure		Head			Remarks
		depth ft	datum ft	measured psi	corrected psi	fresh ft	corr. ft	corr. ft	
T140N R98W									
SunBehn 26-5	sw nw / 26	9152	-6619	4193	----	3065*	2227		
Coastal BN-1	ne ne / 27	9228	-6680	4185	----	2985			
T140N R99W									
Dover Cym.-1	----/ 03	9620	-6896	4199	----	2801			
Farmers 2-13	nw ne / 13	9516	-6889	4364	----	3189*	2766		
T140N R100W									
Conoco Fed. 2-1	sw nw / 02	9781	-7027	4314	----	2936			
Chambers GC 1-8	ne nw / 08	9406	-6827	4347	----	3212*	3052		
Pubco Fed. 22-12	nw sw / 22	9575	-6809	4365	----	3272*	3111		
T140N R102W									
Amerada Mel. 1	sw nw / 30	9103	-6530	4288	----	3383*	3383		
Amerada Mel. 1	sw nw / 30	9422	-6839	4370	----	3254			

APPENDIX B (cont.)

Well Operator/Number	Location spot/section	Gauge		Pressure		Head			Remarks
		depth ft	datum ft	measured psi	corrected psi	fresh ft	corr. ft	corr. ft	
T140N R103W									
Indrex Ryd. 1	se sw / 13	9085	-6585	4216	----	3152			
Indrex Ryd. 1	se sw / 13	9192	-6692	4237	----	3093			
Kewanee Fed. 1	se ne / 13	9153	-6698	4327	----	3295			
Shell St. 1	se / 16	9179	-6561	4318	----	3411*	3411		
Shell Gov. 14-20	sw sw / 20	9185	-6533	4304	----	3407*	3407		
Anadarko A-1	nw sw / 23	9094	-6636	4260	----	3202			
Anadarko A-1	nw sw / 23	9091	-6633	4240	----	3159			
Anadarko A-1	nw sw / 23	9225	-6767	4287	----	3134			
Hunt 1	nw sw / 24	9005	-6553	4242	----	3244			
Hunt A 1	nw ne / 26	9006	-6563	4170	----	3068			
Mesa Fed. 1-35	ne sw / 35	8978	-6484	----	----	----			
Mesa Fed. 1-35	ne sw / 35	8967	-6473	4172	----	3162			
Kissinger 1-36	ne ne / 36	9062	-6543	4280	----	3342*	3342		
T141N R98W									
Adobe 21-6	ne nw / 06	9640	-7043	4361	----	3029			
Adobe 41-6	ne ne / 06	9627	-7030	4465	----	3282			not ss
Gulf Kor. 1	----- / 08	9604	-7026	4409	----	3156*	2559		
Gulf 1-19-1A	nw nw / 19	9580	-6996	4390	----	3143*	2547		
Nucorp 1	se ne / 32	9571	-6855	----	----	----			not ss

APPENDIX B (cont.)

Well Operator/Number	Location spot/section	Gauge		Pressure		Head			Remarks
		depth ft	datum ft	measured psi	corrected psi	fresh ft	corr. ft	corr. ft	
T141N R99W									
Adobe 22-28	se nw / 28	9681	-7007	4268	----	2850			layering
Adobe 23-31	ne sw / 31	9577	-6833	4268	----	3024			
T141N R100W									
Hunt Arm #1	sw nw / 02	9608	-6867	----	----	----			not ss
Al-Aquitaine 1-3	ne nw / 03	9406	-6880	4284	----	3014			
Al-Aquitaine 1-3	ne nw / 03	9389	-6863	4285	----	3033			
Al-Aquitaine 3-3	nw ne / 03	9505	-6906	4097	----	2556			
Shell 41-4	ne ne / 04	9337	-6827	4140	4135	2723			
Al-Aquitaine 1-5	ne nw / 05	9395	-6932	4309	----	3020			
Al-Aquitaine 1-5	ne nw / 05	9350	-6887	3979	----	2302			
Al-Aquitaine 1-5	ne nw / 05	9283	-6820	4336	----	3194			
Getty MC 6-B	sw nw / 06	9270	-6800	4312	4304	3138			
Getty MC B6-13	sw sw / 06	9326	-6826	4049	----	2525			
Al-Aquitaine 1-7	nw nw / 07	9328	-6854	----	----	----			failed
Al-Aquitaine 1-7	nw nw / 07	9320	-6846	4319	----	3129			
Al-Aquitaine 1-7	nw nw / 07	9381	-6907	4359	----	3159			
Shell 33-8	nw se / 08	9364	-6895	4326	----	3096			
Shell 33-8	nw se / 08	9230	-6761	4309	----	3188			
Adobe 14-11	sw sw / 11	9497	-6823	4452	----	3459			
Adobe 12-14	sw nw / 14	9567	-6806	4357	----	3256*	3096	3096a	
Burlington 23-15	ne sw / 15	9354	-6818	4348	----	3224			
Al-Aquitaine 1-16	ne se / 16	9367	-6873	4390	4386	3256			layering not ss

APPENDIX B (cont.)

Well Operator/Number	Location spot/section	Gauge		Pressure		fresh ft	Head		Remarks
		depth ft	datum ft	measured psi	corrected psi		corr. ft	corr. ft	
Al-Aquitaine 1-16	ne se / 16	9300	-6806	4367	4355	3253*	3253	3253a	
Al-Aquitaine 2-16	ne ne / 16	9343	-6797	4286	----	3101			
Al-Aquitaine 1-19	sw se / 19	9336	-6841	4310	----	3112			
Shell 1-2	se ne / 21	9480	-6812	----	----	----			not ss
Al-Aquitaine 1-22	ne ne / 22	9492	-6842	4383	4375	3260			
Al-Aquitaine 2-22	ne sw / 22	9357	-6837	4382	4367	3250*	3250	3250a	
Al-Aquitaine 2-22	ne sw / 22	9338	-6818	4340	4336	3196			
Al-Aquitaine 3-22	se nw / 22	9336	-6819	4371	4363	3256			
Al-Aquitaine 1-23	sw nw / 23	9372	-6827	4267	----	3028			
Al-Aquitaine 1-23	sw nw / 23	9433	-6888	4439	----	3364			not ss
Supron F-26-2	nw sw / 26	9500	-6737	4326	----	3254			
Al-Aquitaine 1-27	se sw / 27	9442	-6804	----	----	----			not ss
Al-Aquitaine 2-27	sw ne / 27	9470	-6789	4261	----	3052			
Al-Aquitaine 2-27	sw ne / 27	9520	-6839	4249	----	2974			
Al-Aquitaine 3-27	se nw / 27	9441	-6748	4514	----	3677			not ss
Al-Aquitaine 1-28	ne ne / 28	9477	-6792	4327	----	3201			
Al-Aquitaine 1-28	ne ne / 28	9469	-6784	4310	----	3170			
Al-Aquitaine 1-30	ne nw / 30	9273	-6803	4377	4369	3286			
Al-Aquitaine 1-30	ne nw / 30	9276	-6806	4359	----	3261*	3261	3261a	
J Chambers 2-31	sw ne / 31	9207	-6718	----	----	----			no build up
J Chambers 2-31	sw ne / 31	9266	-6777	4293	----	3140			
Al-Aquitaine 11-33	ne sw / 33	9238	-6735	----	----	----			not ss
Al-Aquitaine 11-33	ne sw / 33	9290	-6787	4306	----	3158			
Conoco 33-2	ne nw / 33	9302	-6779	4266	----	3073			
Al-Aquitaine 1-33	ne ne / 33	9311	-6782	4341	4336	3232*	3232	3232a	
Mesa FED 1-34	ne nw / 34	9380	-6788	4357	----	3274			poor rec.

APPENDIX B (cont.)

Well Operator/Number	Location spot/section	Gauge		Pressure		Head			Remarks
		depth ft	datum ft	measured psi	corrected psi	fresh ft	corr. ft	corr. ft	
T141N R101W									
Getty MC 1-3	nw nw / 01	9277	-6787	4217	----	2952			
Getty MC 1-3	nw nw / 01	9236	-6746	4185	----	2919			
Getty MC 1-1	ne ne / 01	9229	-6773	4365	4355	3284*	3125	3125a	
Getty MC 1-11	ne sw / 01	9267	-6749	4341	----	3276*	3116	3116a	
Tenneco Oyhus 1-2	sw nw / 02	9103	-6756	4171	----	2877			
Coastal BN 1	ne se / 03	9165	-6765	3449	----	1200			
Al-Aquitaine 3-11	se ne / 11	9297	-6777	4096	----	2687			
Al-Aquitaine 4-11	ne nw / 11	9304	-6804	4140	----	2757			
Al-Aquitaine 1-11	ne sw / 11	9330	-6825	4333	----	3182			
J Chambers 4-12	nw nw / 12	9317	-6821	4352	----	3230			
J Chambers 4-12	nw nw / 12	9328	-6832	4362	----	3242			
Al-Aquitaine ST-1	se nw / 13	9105	-6510	4371	----	3432			not MC
Al-Aquitaine ST-1	se nw / 13	9413	-6818	4363	----	3267*	3267	3267a	
Chambers 2-14X	se se / 14	9253	-6752	4015	----	2521			
Al-Aquitaine 1-14	ne ne / 14	9494	-6834	4325	4320	3143			
Al-Aquitaine 1-14	ne ne / 14	9479	-6819	4315	----	3146			
Al-Aquitaine 2-14	ne nw / 14	9342	-6750	4130	----	2783			
Chambers FCS 1-14	ne sw / 14	9360	-6857	4356	----	3203			
Chambers ST-2-14X	se se / 14	9285	-6784	4046	----	2560			
Chambers ST-2-14X	se se / 14	9305	-6804	4031	----	2505			
Chambers ST-2-14X	se se / 14	9404	-6903	4092	----	2547			
Chambers ST-1-15	se se / 15	9241	-6805	4340	4334	3204			
Chambers ST-1-15	se se / 15	9249	-6813	4340	4334	3196			
Chambers NDST-1-22	sw ne / 22	9266	-6867	4365	----	3213*	3213	3212a	

APPENDIX B (cont.)

Well Operator/Number	Location spot/section	Gauge		Pressure		fresh ft	Head		Remarks
		depth ft	datum ft	measured psi	corrected psi		corr. ft	corr. ft	
Chambers FCS-1-23	ne nw / 23	9234	-6730	4320	4315	3236*	3236	3236a	
Chambers NDST-2-23	se ne / 23	9360	-6861	4319	----	3114			
Chambers ST-4-23	se sw / 23	9160	-6814	4310	----	3140			
Al-Aquitaine 3-24	nw sw / 24	9304	-6822	4360	4355	3247*	3247	3247a	
Al-Aquitaine 1-24	se ne / 24	9325	-6811	4290	----	3108			
Al-Aquitaine 4-24	nw nw / 24	9351	-6853	4153	----	2738			
Patrick M-1-25	sw nw / 25	9160	-6776	4361	----	3295			poor rec.
Patrick H-1-27	nw se / 27	9248	-6731	4264	----	3117			
Patrick H-1-27	nw se / 27	9260	-6753	4150	----	2831			
Patrick H-2-27	sw nw / 27	9170	-6758	3721	----	1836			
Patrick H-3-27	se ne / 27	9276	-6820	4035	----	2499			
Patrick H-4-27	nw sw / 27	9271	-6755	3953	----	2374			
T141N R102W									
Al-Aquitaine 1-9	ne sw / 09	9237	-6770	4398	----	3387*	3225		
Al-Aquitaine 1-10	sw sw / 10	9161	-6743	4381	----	3375			
Cenex FED-12-29	nw sw / 29	9227	-6610	4297	----	3314*	3314		
Cenex FED-12-29	nw sw / 29	9270	-6653	4301	----	3280			
Patrick H-F 1-30	ne se / 30	9175	-6572	4277	----	3306			
T142N R98W									
Anadarko REP-A-1	sw se / 03	9868	-7100	4474	----	3232*	2339		
Adobe STR-34-31	sw se / 31	9561	-6946	4274	----	2995			
Gulf SSL-2-36	nw sw / 36	9646	-6972	4458	----	3324			poor rec.

APPENDIX B (cont.)

Well Operator/Number	Location spot/section	Gauge		Pressure		Head			Remarks
		depth ft	datum ft	measured psi	corrected psi	fresh ft	corr. ft	corr. ft	
Gulf SSL-2-36	nw sw / 36	9975	-7301	4498	----	3088*	2188		
		T142N R99W							
Hunt Baranko-1	nw ne / 03	9863	-7135	4512	----	3285*	2364		
		T142N R100W							
Koch FED-6-3	se nw / 03	9745	-6942	4316	----	3026			
Koch FED-7-3	sw ne / 03	9730	-6952	3874	----	1995			
Hunt R-A-1	se se / 04	9776	-6963	4196	----	2728			
Hunt R-A-1	se se / 04	9756	-6943	4248	----	2868			
Koch Kordon-4-5	sw sw / 05	9604	-6882	4307	4300	3045			
Koch FED-6-6M	se nw / 06	9605	-6854	4161	----	2756			
Koch FED-6-6M	se nw / 06	9687	-6936	4287	----	2965			
Koch FED-10-6	nw se / 06	9670	-6980	4020	4017	2304			
Koch FED-K-15-6	sw se / 06	9596	-6849	3833	----	2003			
Brown FED-8-12X	nw nw / 08	9525	-6886	3842	----	1987			
Brown FED-8-12X	nw nw / 08	9467	-6828	3854	----	2080			
Supron SND-1	sw ne / 09	9618	-6861	4220	----	2885			
Supron SND-1	sw ne / 09	9609	-6852	4041	----	2481			barrier
Hunt Gregory-1	sw ne / 10	9660	-6878	4380	----	3237*	2812	2812a	
Hunt Osadchuch-2	se se / 15	9624	-6881	4339	----	3140			layering
Hunt Fritz-1	ne ne / 22	9547	-6797	4379	4365	3285			
Hunt Fritz-1	ne ne / 22	9680	-6930	4378	----	3180			
Hunt Osadehuk	sw nw / 23	9611	-6871	4394	4384	3254*	2828	2705a	

APPENDIX B (cont.)

Well Operator/Number	Location spot/section	Gauge		Pressure		Head			Remarks
		depth ft	datum ft	measured psi	corrected psi	fresh ft	corr. ft	corr. ft	
Hunt Anheluk-ST-2	sw se / 23	9670	-----	-----	-----	-----			failed
Patrick 1-26	sw nw / 26	9689	-6933	4412	-----	3256			
Koch FED-1-27	ne ne / 27	9618	-6905	4225	-----	2853			
Patrick FED-2-28	sw ne / 28	9526	-6895	3565	-----	1338			
Supron NDST-2	ne sw / 28	9621	-6904	3465	-----	1098			
Koch FED-10-31	nw se / 31	9309	-6859	4213	-----	2871			
Patrick FED-2-32	sw nw / 32	9406	-6920	4281	-----	2966			
Patrick FED-2-32	sw nw / 32	9281	-6795	4355	-----	3263			
Patrick FED-1-32	ne sw / 32	9281	-6819	4117	-----	2689			
Koch FED-1-33	sw ne / 33	9345	-6832	4362	-----	3242*	2818	2818a	
Supron Cerkoney-3	nw se / 34	9460	-6812	4283	4273	3056			
Supron Cerkoney-1	nw sw / 34	9432	-6852	4358	4350	3195			
Supron Cerkoney-4	nw ne / 34	9565	-6906	4347	-----	3160			
Supron FED-1-35	ne sw / 35	9660	-6923	4413	-----	3269*	2840	2840a	
Supron FED-2-35	nw sw / 35	9637	-6889	4248	-----	2922			
Supron FED-3-35	nw nw / 35	9606	-6832	4101	-----	2639			
T142N R101W									
Anderson FED-1-1	ne se / 01	9570	-6907	3324	-----	770			
Conoco FED-H-8-1	ne se / 08	9286	-6856	4411	-----	3331*	2913	2913a	
Brent FED-11	ne sw / 08	9325	-6880	4412	-----	3310*	2875	2875a	
Koch FED-16-14	se se / 14	9350	-6828	-----	-----	-----			
Coastal BN-1	se se / 15	9310	-6809	3286	-----	780			
Coastal BN-3	se nw / 23	9520	-6832	3629	-----	1543			
Milestone BN-23-23	ne sw / 23	9389	-6845	3027	-----	146			

APPENDIX B (cont.)

Well Operator/Number	Location spot/section	Gauge		Pressure		Head			Remarks
		depth ft	datum ft	measured psi	corrected psi	fresh ft	corr. ft	corr. ft	
Milestone BN-23-23	ne sw / 23	9400	-6856	3026	----	132			
Koch FED-8-24	se ne / 24	9357	-6835	4303	4296	3086			
Koch FED-9-24	ne se / 24	9335	-6877	4291	----	3033			layering
Koch FED-13-24	sw sw / 24	9352	-6809	4158	----	2794			
Getty MC-A-36-10	nw ne / 36	9340	-6810	4336	----	3190			
T142N R102W									
Shamrock FED-34-4	sw se / 04	9147	-6591	4331	----	3411			
Shamrock RS-21-9	sw se / 04	9367	-6811	4402	----	3355			
Mackoff 23-17	ne nw / 09	9403	-6867	4452	----	3415*	3255		
Mackoff 23-17	ne sw / 17	9465	-6859	4436	----	3386			
Cenex FED-14-26	ne sw / 17	9389	-6783	4414	----	3420*	3258		
T143N R98W									
Amoco 1-1	ne ne / 04	9731	-7256	4467	----	3060			
Amoco 1-1	----- / 28	9891	-7199	4512	----	3221*	2320		
Amarex Krogh-1	sw nw / 34	9795	-7103	4452	----	3179			
Mosbacher GS-1-36	ne nw / 36	9812	-7122	4488	----	3242			
Mosbacher GS-1-36	ne nw / 36	9743	-7053	4462	----	3253*	2360		
T143N R99W									
Amoco Hecker-1	-----/ 02	9922	-7205	4524	----	3243*	2349		
Amoco 1-1	se se / 09	9851	-7109	4480	----	3237*	2342		layering

APPENDIX B (cont.)

Well Operator/Number	Location spot/section	Gauge		Pressure		Head			Remarks
		depth ft	datum ft	measured psi	corrected psi	fresh ft	corr. ft	corr. ft	
Amoco Knudtson-1	ne ne / 21	9880	-7150	4490	----	3220*	2332		
Hunt Demanion-1	se sw / 34	9919	-7172	4529	----	3287			
T143N R100W									
Al-Aquitaine BN5-1	se nw / 05	9292	-6874	4484	----	3482			not ss
Al-Aquitaine 1-8	nw ne / 08	9418	-6957	4645	----	3770			not ss
Al-Aquitaine 1-8	nw ne / 08	9460	-6999	4459	----	3299*	2529		
Davis J-FED-1	se se / 08	9638	-6932	4391	----	3209			
Al-Aquitaine 1-16	se se / 16	9728	-7009	4207	----	2707			
Gulf DC-1-18-1A	nw nw / 18	9681	-6932	4474	----	3400			poor rec.
Gulf DC-1-18-1A	nw nw / 18	9754	-7005	4533	----	3464			not ss
Everett FED-5-22	sw nw / 22	9665	-6929	4241	----	2865			
Coastal Y-23-1	nw nw / 23	9550	-6951	4360	----	3118			
Hunt Johnson-1	nw se / 27	9660	-6959	4152	----	2637			
Tenneco BN-1-29	ne sw / 29	9556	-6914	4425	----	3305*	2705	2543a	
Tenneco G-1-30	se ne / 30	9468	-6856	4440	----	3398			not ss
Tenneco FED-2-30	se se / 30	9568	-6891	4414	----	3303*	2703	2540a	
Apache BN-2-31B	sw se / 31	9683	-6927	3822	----	1900			
Koch Simmioniw-2	nw se / 32	9573	-6857	4320	----	3120			
Koch Simmioniw-1	sw ne / 32	9598	-6896	4349	----	3148			
Hunt Kordon-2	nw sw / 32	9562	-6826	4266	----	3026			
Farmers FED-4-33	nw nw / 33	9531	-6851	4400	----	3310*	2883	2551a	layering
Koch FED-5-33	sw nw / 33	9617	-6827	3904	----	2189			
Patrick H-1-34	sw sw / 34	9412	-6689	4358	----	3375			not MC?
Koch FED-15-34	sw se / 34	9615	-6873	4076	----	2540			

APPENDIX B (cont.)

Well Operator/Number	Location spot/section	Gauge		Pressure		Head			Remarks
		depth ft	datum ft	measured psi	corrected psi	fresh ft	corr. ft	corr. ft	
Hunt Fedora-1	nw ne / 34	9665	-6919	4086	----	2517			
		T143N R101W							
Samson FED-1-2	sw sw / 02	9389	-7016	4450	----	3261*	2492		
Farmers FED-11-4	ne sw / 04	9372	-6943	4296	----	2978			
Farmers FED-11-4	ne sw / 04	9312	-6883	4197	----	2810			
Apache FED-13-4	sw sw / 04	9318	-6965	4152	----	2624			
Cenex FED-2-4	nw ne / 04	9377	-6922	3923	----	2138			
Apache 1-8	ne se / 08	9366	-6911	4255	----	2916			
Apache 1-9	ne sw / 09	9401	-6956	4245	----	2848			
Cenex Fed-12-10	nw sw / 10	9398	-6922	3611	----	1417			
Apache ST-1-16	ne sw / 16	9468	-6975	4355	----	3083			
Apache ST-4-16	nw se / 16	9451	-6950	4134	----	2597			
Apache ST-3-16	nw ne / 16	9515	-6989	4038	----	2337			
Apache Fed-4-17	sw sw / 17	9409	-6965	4144	----	2605			
Apache FED-4-17	sw sw / 17	9372	-6928	4287	----	2973			
Chambers BFED-3-19	sw sw / 19	9302	-6929	4408	----	3251			
Tenneco BN-1-25	nw nw / 25	9537	-6982	4436	----	3263*	2661	2497a	
Chambers BU-2-27	sw sw / 27	9366	-6876	4435	----	3366			
Chambers BFED-1-28	se nw / 28	9405	-6990	4494	----	3388*	2765	2612a	
		T143N R102W							
Cenex BN-5-1	sw nw / 01	9233	-6933	4312	----	3025			
Cenex Connell-6-2	se nw / 02	9196	-6919	4318	----	3053			

APPENDIX B (cont.)

Well Operator/Number	Location spot/section	Gauge		Pressure		Head		Remarks
		depth ft	datum ft	measured psi	corrected psi	fresh ft	corr. ft	
Cenex Connell-6-2	se nw / 02	9255	-6978	4368	----	3110		
Apache FED-1-5	ne se / 05	9150	-6995	4409	----	3187		
Conoco FEDB-13-1	se se / 13	9270	-6926	4198	----	2769		
N.A.Royalties-1-3	se se / 22	9289	-6939	4404	----	3232		
Al-Aquitaine BN-23	---- / 23	9226	-6916	4429	----	3306*	2883	
T143N R103W								
Grace FED-52-22	sw ne / 22	9315	-6860	4338	----	3158		
Payette BC-24-23	---- / 24	9360	-6830	4383	----	3292		
Shamrock W-F-24-25	se sw / 25	9372	-6777	4432	----	3459		
Shamrock W-F-24-25	se sw / 25	9397	-6802	4430	----	3429*	2998	
Shamrock W-F-24-25	se sw / 25	9427	-6832	4425	----	3387		
Gas Prod. ST-1-1	nw nw / 36	9356	-6832	4451	----	3447		
Gas Prod. ST-2	ne se / 36	9283	-6813	4352	----	3238		
T144N R98W								
Gulf Miller #1-10	nw se / 10	9760	-7182	4535	4523	3265*	2360	
T144N R99W								
Amoco Tachenko #1	se se / 14	9923	-7182	4542	----	3308*	2400	
Supron H-D 1	sw ne / 21	9880	-7164	4512	----	3256*	2355	
Amoco B1	nw se / 29	9834	-7158	4463	----	3149		

APPENDIX B (cont.)

Well Operator/Number	Location spot/section	Gauge		Pressure		Head			Remarks
		depth ft	datum ft	measured psi	corrected psi	fresh ft	corr. ft	corr. ft	
T144N R100W									
Patrick 1-4	sw ne / 04	9688	-7216	4512	----	3204			
Patrick 1-4	sw ne / 04	9818	-7346	4585	----	3245*	2326		
Amoco Fed.1	se nw / 20	9523	-6965	4482	----	3386*	2490		
Koch Fed. 13-30	sw sw / 30	9657	-7042	4457	----	3251*	2360		
Koch Fed. 13-30	sw sw / 30	9577	-6962	4422	----	3250			
Koch Fed. 13-30	sw sw / 30	9513	-6898	4458	----	3398			ss ?
Apache Fed. 33-31	nw se / 31	9410	-7007	4397	----	3148			
Apache Fed.33-31	nw se / 31	9545	-7142	----	----	---			not ss
Jordan 1-1	se se / 36	9759	-7162	4509	----	3251			
Jordan 1	se se / 36	9789	-7192	4535	----	3281*	2375		
T144N R101W									
Supron 6-3	nw se / 06	9248	-7045	4302	----	2890			
Supron 6-2	se ne / 06	9188	-6977	4205	----	2734			
Supron 7-1	nw ne / 07	9229	-6979	4305	----	2963			
Supron 7-1	nw ne / 07	9289	-7039	4348	----	3002			erratic
Florida 8-2	ne nw / 08	9285	-7024	4392	----	3119			
Florida 8-3	ne nw / 08	9251	-6990	4443	----	3271*	2384		
Koch 6-11	se nw / 11	9330	-7005	4412	----	3184			
Koch 6-11	se nw / 11	9392	-7067	4412	----	3122			barrier
Northrop Al-13	sw sw / 13	9434	-7103	4411	----	3084			
Northrop Al-13	sw sw / 13	9441	-7110	4498	----	3278*	2501		
Amoco F-2	se sw / 15	9315	-6977	4326	----	3014			

APPENDIX B (cont.)

Well Operator/Number	Location spot/section	Gauge		Pressure		Head			Remarks
		depth ft	datum ft	measured psi	corrected psi	fresh ft	corr. ft	corr. ft	
Amoco F-2	se sw / 15	9408	-7060	4372	----	3037			
Duncan 15-43	ne se / 15	9367	-7012	4306	----	2933			
Supron 18-1	sw ne / 18	9484	-7211	4350	----	2835			
Supron 19-1	se sw / 19	9218	-6970	4292	----	2942			
Florida 19-1	se sw / 19	9270	-7022	4291	----	2886			layering
Koch 6-22	se nw / 22	9386	-7023	4317	----	2947			
Koch 6-22	se nw / 22	9407	-7044	4369	----	3046			
Koch 13-22	sw sw / 22	9576	-6991	4342	----	3037			
Tenneco 2-28	se sw / 28	9214	-6944	4151	----	2543			
Ladd 34-11	nw nw / 34	9319	-7001	3990	----	2215			
T144N R102W									
MGF 44-1	se se / 01	9302	-6994	4358	----	3071			
MGF 44-1	se se / 01	9357	-7049	4319	----	2926			
MGF 42-1	se ne / 01	9219	-6986	4220	----	2760			
Apache 2-4	sw sw / 02	9520	-6996	4124	----	2528			
Apache 2-4	sw sw / 02	9624	-7100	4244	----	2701			
Texakota 1-2	nw ne / 02	9295	-7041	4335	----	2971			
Texakota 1-2	nw ne / 02	9303	-7049	4359	----	3018			
Apache 2-5	sw ne / 02	9460	-7065	4038	----	2261			
Apache 3-2A	sw sw / 03	9263	-7029	4242	----	2768			
Apache 3-2A	sw sw / 03	9308	-7074	4247	----	2761			
Apache 3-1	ne ne / 03	9386	-6865	4069	----	2532			
Apache 3-1	ne ne / 03	9488	-6967	4135	----	2583			
Supron F-1	ne se / 10	9549	-7342	4297	----	2582			

APPENDIX B (cont.)

Well Operator/Number	Location spot/section	Gauge		Pressure		Head			Remarks
		depth ft	datum ft	measured psi	corrected psi	fresh ft	corr. ft	corr. ft	
Supron F-1	ne se / 10	9632	-7425	4393	----	2720			
Florida 13-1	ne ne / 13	9665	-6976	4254	----	2848			
Apache 2-14	sw sw / 14	9189	-6952	4361	----	3120			
Apache 2-14	sw sw / 14	9198	-6961	4323	----	3023			
Apache 15-1	ne se / 15	9218	-6951	4219	----	2793			
Apache 15-2	ne ne / 15	9490	-6969	4186	----	2698			
Apache 22-1	ne se / 22	9265	-6969	4331	----	3033			
Apache 22-1	ne se / 22	9260	-6964	4338	----	3054			
Apache 1-22	ne ne / 22	9153	-6980	4422	----	3232			
Apache 1-22	ne ne / 22	9230	-7057	4456	----	3234			
Apache 2-23	sw nw / 23	9092	-6916	4440	----	3338			
Apache 2-23	sw nw / 23	9204	-7028	4444	----	3235			
Apache 2-23	sw nw / 23	9142	-6966	4438	----	3283*	2396		
Apache 23-3	ne sw / 23	9162	-6987	4109	----	2503			
Apache 23-3	ne sw / 23	9189	-7014	4056	----	2353			
Apache 23-3	ne sw / 23	9184	-7009	4039	----	2319			
Apache 27-1	sw ne / 27	9224	-7026	4425	----	3193			
Apache 27-1	sw ne / 27	9165	-6957	4500	----	3436			
Apache 27-1	sw ne / 27	9149	-6941	4466	----	3373*	2480		
Coastal 1-29	nw nw / 29	9206	-6967	4353	----	3086			

VITA

NAME: Alan Ray Mitsdarffer

BIRTHDATE: October 22, 1954

BIRTHPLACE: Champaign, Illinois

PARENTS: Charles A. and Maxine Mitsdarffer

EDUCATION: College of William and Mary
Williamsburg, Virginia
B.S., 1976, Geology

PROFESSIONAL
MEMBERSHIPS: AAPG

EMPLOYMENT: Century Geophysical Corp.
Contract Field Geologist
Phillips Coal Company
Pennzoil (present)

PERMANENT
ADDRESS: 15842 Timber Rock Dr.
Houston, Texas 77082

7611 226